NUSC Technical Report 8747
31 July 1990

(2)

Reduced Dimension Adaptive Beamforming

Douglas A. Abraham
Antisubmarine Warfare
Systems Department

Naval Underwater Systems Center
Newport, Rhode Island / New London, Connecticut

Preface

This document was prepared under NUSC project number 633W20 and was funded by the Naval Underwater Systems Center, New London, CT.

The author wishes to thank those who helped to review and refine this document, among them are Norman Owsley, Robert Turner, Charles Knapp, and Donald Abraham.

The technical reviewer for this document was N. Owsley (Code 2121).

Reviewed and Approved: 31 July 1990

D. W. Counsellor
Head, Antisubmarine Warfare Systems Department

REPORT DOCUMENTATION PAGE

Form Approved
OMB No. 0704-0188

1. AGENCY USE ONLY (Leave blank)	2. REPORT DATE	3. REPORT TYPE AND DATES COVERED
	31 July 1990	Final

4. TITLE AND SUBTITLE

REDUCED DIMENSION ADAPTIVE BEAMFORMING

5. FUNDING NUMBERS

NUSC PR 633W20

6. AUTHOR(S)

Douglas A. Abraham

7. PERFORMING ORGANIZATION NAME(S) AND ADDRESS(ES)

Naval Underwater Systems Center
New London Laboratory
New London, CT 06320

8. PERFORMING ORGANIZATION REPORT NUMBER

TR 8747

9. SPONSORING/MONITORING AGENCY NAME(S) AND ADDRESS(ES)

10. SPONSORING/MONITORING AGENCY REPORT NUMBER

11. SUPPLEMENTARY NOTES

12a. DISTRIBUTION/AVAILABILITY STATEMENT

Approved for public release; distribution is unlimited.

12b. DISTRIBUTION CODE

13. ABSTRACT (Maximum 200 words)

This document contains material used in a Thesis submitted in partial fulfillment of the requirements for the Degree of Master of Science at the University of Connecticut.

14. SUBJECT TERMS

Adaptive Beamforming

15. NUMBER OF PAGES

112

16. PRICE CODE

17. SECURITY CLASSIFICATION OF REPORT	18. SECURITY CLASSIFICATION OF THIS PAGE	19. SECURITY CLASSIFICATION OF ABSTRACT	20. LIMITATION OF ABSTRACT
UNCLASSIFIED	UNCLASSIFIED	UNCLASSIFIED	UL

TABLE OF CONTENTS

		Page
LIST OF FIGURES		iii
LIST OF TABLES		vi
CHAPTER 1	INTRODUCTION	
1.0	Problem Formulation	1
1.1	Current Technology	3
CHAPTER 2	BEAMFORMING BACKGROUND	
2.0	Introduction	5
2.1	Array Signal Processing	5
2.2	Beamforming	6
2.3	Time and Frequency Domain Beamformers	7
2.4	Sensor Array Geometry	7
2.5	Conventional Beamforming	9
2.6	Adaptive Beamforming	10
2.7	Reduced Dimension Adaptive Beamforming	12
CHAPTER 3	THEORY	
3.0	Introduction	14
3.1	Models and Assumptions	14
3.2	Conventional Beamforming	19
3.3	Matrix Preprocessed MVDR	27
3.3.1	Subarray Preprocessing	36
3.3.1.1	Wavenumber Analysis	38

3.3.1.2	Subarrays	42
3.3.2	Beam Space Preprocessing	51
3.4	Enhanced Minimum Variance Beamforming	53
CHAPTER 4	COMPARISON	
4.0	Introduction	58
4.1	Array Gain Improvement	58
4.2	Beampatterns	67
4.3	Beam Responses	69
4.4	Numerical Intensity	87
CHAPTER 5	CONCLUSIONS	
5.1	Summary	89
5.2	Future Work	91
APPENDIX		
A	Cross Spectral Density Matrix Update and Inversion	95
B	Eigen-structure Estimation	99
C	Subarray Sizing Algorithm	101
REFERENCES		105

LIST OF FIGURES

		Page
2.1	Frequency domain beamformer	8
2.2	Line array with point source at angle theta	9
2.3	Conventional beamformer beampattern	10
3.1	Pre-beamformer signal path	15
3.2	Delay between adjacent sensors	16
3.3	Uniform CBF beampattern steered to 30 degrees	23
3.4	Chebyshev CBF beampattern with 30dB sidelobes	24
3.5	CBF beam response with uniform shading	26
3.6	CBF beam response with 30dB Chebyshev shading	27
3.7	Matrix preprocessor - ABF configuration	28
3.8	Full array partitioned into subarrays	37
3.9	Wavenumber spectrum	43
3.10	Beampattern applied to wavenumber spectrum	44
3.11	Beampattern aliasing with spectrum	45
3.12	Beampattern aliasing	46
3.13	Subarray spacing example	48
3.14	Scalloping loss limit on mainlobe of beampattern	50
3.15	Spacing of subarray beams in wavenumber	50
4.1	Array gain improvement (AGI) for a mainlobe point interference (PIN) with high signal-to-interference ratio	63
4.2	Array gain improvment (AGI) for a mainlobe point interference (PIN) with low signal-to-interference ratio	64

4.3 Array gain improvement (AGI) for a sidelobe point interference (PIN) with intermediate signal-to-interference ratio 65
4.4 CBF beampattern, uniform shading, all arrival angles .. 70
4.5 CBF beampattern, uniform shading, selected arrival angles 70
4.6 MVDR beampattern, all arrival angles 71
4.7 MVDR beampattern, selected arrival angles 71
4.8 Subarray beampattern, all arrival angles 72
4.9 Subarray beampattern, selected arrival angles 72
4.10 Beam space beampattern, all arrival angles 73
4.11 Beam space beampattern, selected arrival angles 73
4.12 EMVDR beampattern, one eigenvector, all arrival angles .. 74
4.13 EMVDR beampattern, one eigenvector, selected arrival angles 74
4.14 EMVDR beampattern, two eigenvectors, all arrival angles 75
4.15 EMVDR beampattern, two eigenvectors, selected arrival angles 75
4.16 Beam response - Single source 82
4.17 Beam response - Single source, mainlobe interference, SIR = -10dB 83
4.18 Beam response - Single source, sidelobe interference, SIR = -10dB 84
4.19 Beam response - Single source, mainlobe interference, SIR = -3dB 85

4.20 Beam response - One stationary source, one moving source 86

LIST OF TABLES

		Page
3.1	Functions to be extremized as related to various optimal conditions	34
4.1	Array gain improvement (AGI) for full array MVDR and beam space, subarray and EMVDR reduced dimension beamformers	63
4.2	Beamformer configurations for Figures 4.4 - 4.15	68
4.3	Beam response case scenario descriptions	78
4.4	Plane wave source deflections (dB) for beamformer outputs	79
4.5	Beamformer complexity expressed in number of arithmetic operations per update	87
4.6	Numerical gain for beamformers of Section 4.3	88

CHAPTER 1 - INTRODUCTION

1.0 Problem Formulation

Adaptive methods of beamforming that yield high resolution beam outputs require a much greater numerical intensity than conventional Fourier techniques of beamforming. Reduction of the adaptive dimension of these data dependent beamformers can alleviate the numerical intensity problem with a negligible loss in performance.

The adaptive dimension reduction may be accomplished by a matrix premultiplication of the array sensor data. The matrix premultiplication, known as matrix preprocessing, transforms the N dimension array data vector into an M dimensional space where $M < N$. The M dimensional data is then beamformed with a minimum variance distortionless response (MVDR) adaptive beamformer.

Another method of reducing the adaptive dimension is by the approximation of the covariance or cross spectral density matrix (CSDM) by its dominant or strongest eigenvectors. This technique, developed by Owsley in [1] and [10], is known as the enhanced minimum variance beamformer (EMVDR).

The intent of this thesis is to present and compare the matrix preprocessor configuration and the enhanced minimum variance

reduced dimension adaptive beamformers. The subarray and beam space matrix preprocessors will be covered. The comparison will be against a full array MVDR beamformer and a conventional beamformer.

A general introduction to the concept, application and implementation of beamforming is covered in Chapter 2. Conventional and adaptive methods of beamforming are discussed and the reduced dimension adaptive beamformer is proposed.

The models and assumptions used in the development of the beamformers are presented in Section 3.1. Conventional beamforming, the beamformer beampattern and beam response are covered in Section 3.2. The matrix preprocessed MVDR algorithm development, subarray and beam space preprocessors and a discussion of wavenumber analysis are covered in Section 3.3. The enhanced minimum variance beamformer is developed in Section 3.4.

The comparisons will first be in the form of a metric introduced by Owsley in [4] and [10] called the Array Gain Improvement (AGI) in Section 4.1, then beampatterns in Section 4.2, followed by beam responses in Section 4.3 and numerical intensity in Section 4.4.

The significant contributions of this thesis include the exploration of the subarray matrix preprocessor and the stochastic evaluation of the beamformers.

1.1 Current Technology

Adaptive algorithms have origins dating to the 1960's. The numerical intensity required of the implementation has always been a hurdle that required surmounting. Alternatively the use of sub-optimal techniques has been proposed in [11]. With the onslaught of VLSI technology, realization of broadband full array adaptive beamformers has become a reality. For a fixed amount of processing power a trade-off exists between the size of the array, the number of beams and the number of frequencies the beamformer operates on.

The MVDR algorithm was first developed with a soft distortionless response constraint by Owsley [17] in 1969 and with a hard constraint as shown by Frost [18] in 1972.

The reduced dimension adaptive beamformers to be discussed have been proposed by various people. The subarray preprocessor was alluded to by Owsley in [2], the beam space preprocessor by Gray in [3] and the enhanced minimum variance beamformer was developed by Owsley in [1] and [10]. Several others have worked with the reduced adaptive dimension idea as comprehensively shown in [12] by Van Veen.

The implementation of the subject beamformers requires two specialized algorithms. The first is used to realize the covariance matrix inversion for the MVDR beamformer via the Cholesky square root factor and is found in [2] and [5]. The second is an eigenvector and eigenvalue estimator used to compute the eigen-decomposition of the covariance matrix for the EMVDR beamformer and is developed by Yang and Kaveh in [7]. The Cholesky square root factor CSDM exponential update and inverse and the eigenvector algorithm by Yang and Kaveh are respectively shown in Appendices A and B.

CHAPTER 2 - BEAMFORMING BACKGROUND

2.0 Introduction

The intent of this section is to introduce the reader to the concept of beamforming, its uses, implementations and structures. The properties of conventional and adaptive beamforming are discussed and the concept of reduced dimension adaptive beamforming is proposed.

2.1 Array Signal Processing

Array signal processing consists of the processing methods used to analyze the signals received from an array or group of transducers. The signals arriving at the array are traveling waves of differing frequencies and arrival angles. Applications of array signal processing may be found in seismology, radar, sonar, and other fields as seen in [1]. Examples of sensor arrays include sensors measuring seismic activity in the earth, radar antennae and underwater transducers sensing pressure waves. The signals received by the sensors are used to estimate parameters associated with the sources causing the traveling waves. The parameters may include frequencies, amplitudes, relative phase delays, angles of arrival, source location, etc. Beamforming is an array signal processing technique that aids in the estimation of these parameters and in the detection of the traveling waves.

2.2 Beamforming

Beamforming combines the data from the array sensors into a single "beam" output. Several beams are computed so that they "look" in directions that span the possible arrival angles of an impinging traveling wave. The directional aspect of beamforming is accomplished by the attenuation and phasing or delay of signals coming from different directions. This process may be related to a bandpass finite impulse response (FIR) filter operating on time series data. The transfer function of the filter is similar to the beamformer's beampattern where different directions are attenuated instead of frequencies. The beampattern is discussed more thoroughly in Section 3.2. A beamformer is thus also known as a spatial filter. The relations between spectral estimation and beamforming will be exploited when possible to assist the reader in relating the text to a familiar topic.

Other characteristics of beamforming include the increase in signal to noise ratio (SNR) at the output of a beam as compared to the SNR at a single sensor. The ratio of the beam output SNR to the sensor level SNR is known as the array gain [8]. As in frequency estimation the angle of arrival or spatial frequency of a traveling wave may be found by forming several beams and estimating the spatial spectrum.

2.3 Time and Frequency Domain Beamformers

Beamforming may be accomplished in either the time domain where the sensor outputs are delayed, scaled and summed or in the frequency domain where the delay operation translates, via a Fourier transform, into a phase shift. The phase shift of the frequency domain beamformer is accomplished by the multiplication of a frequency dependent complex exponential.

The time domain beamformer operates on all frequencies and is thus wideband. A frequency domain beamformer first converts each sensor output time signal into the frequency domain by a Fast Fourier Transform (FFT). The sensor outputs at discrete frequencies bins are then scaled, phase shifted and summed to form a single frequency beam output. The beamforming is thus performed over a frequency band as wide as an FFT bin. If several frequency bins are beamformed and converted back into the time domain by an inverse FFT (IFFT), then time domain beam outputs are available. Figure 2.1 describes the frequency domain beamformer which will be the implementation discussed in this paper.

2.4 Sensor Array Geometry

Without a loss of generality we will restrict the configuration of the sensor arrays used as examples to be a set of equally spaced sensors placed in a straight line. This may be directly related to the uniform time sampling performed on a voltage or current waveform. In this case the waveform being sampled is the signal field impinging

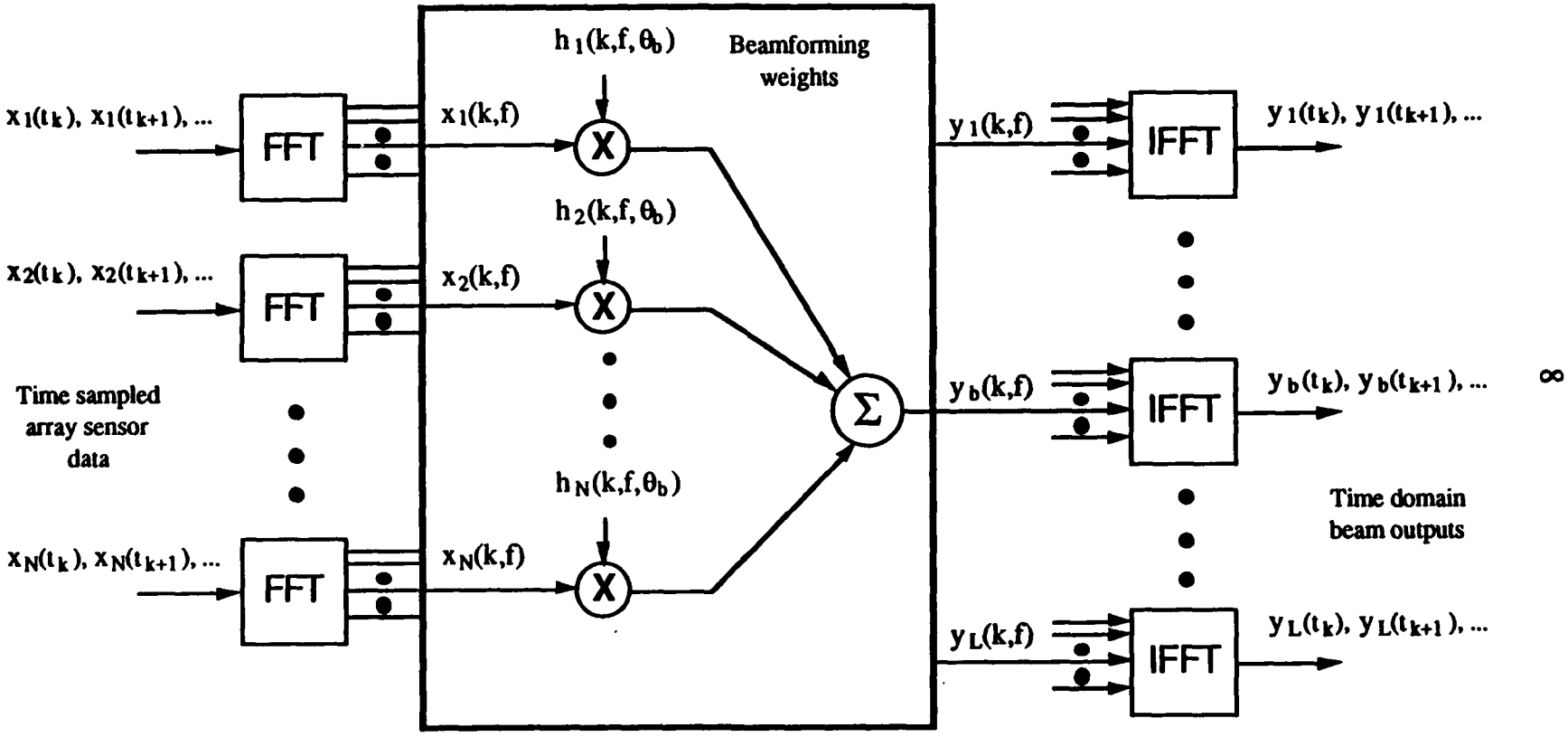

Figure 2.1 Frequency domain beamformer.

on the sensor array. The sources generating the traveling waves are assumed to be point sources and the propagation of the waves istaken to be spherical. Figure 2.2 depicts a line array of sensors with a point source emitting a wave impinging on the array. The perpendicular direction to the line array is known as "broadside". From broadside traveling waves may arrive at the array in angles ranging from -90 to +90 degrees.

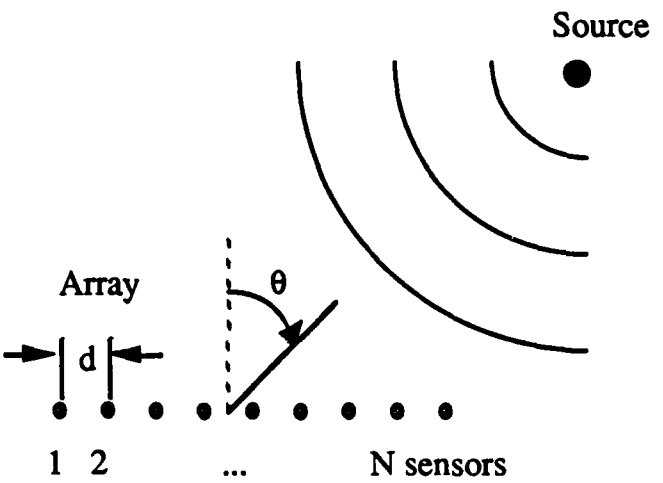

Figure 2.2 Line array with point source at angle theta.

2.5 Conventional Beamforming

Conventional beamforming (CBF) is beamforming with the use of fixed amplitude scalings and phase shifts. This provides a constant beampattern that depends on the scalings used and the total length or aperture of the array. This is the most widely accepted type of beamforming. The spectral estimation analog of CBF is the discrete fourier transform (DFT) or periodogram method with amplitude shading of the data. Marple calls this the Welch

periodogram in [9]. Figure 2.3 shows a typical beam pattern plot. The pointing direction of the beam, commonly called the main response axis (MRA) or the angle the beam is steered to, is the angle at which an incoming signal receives no degradation.

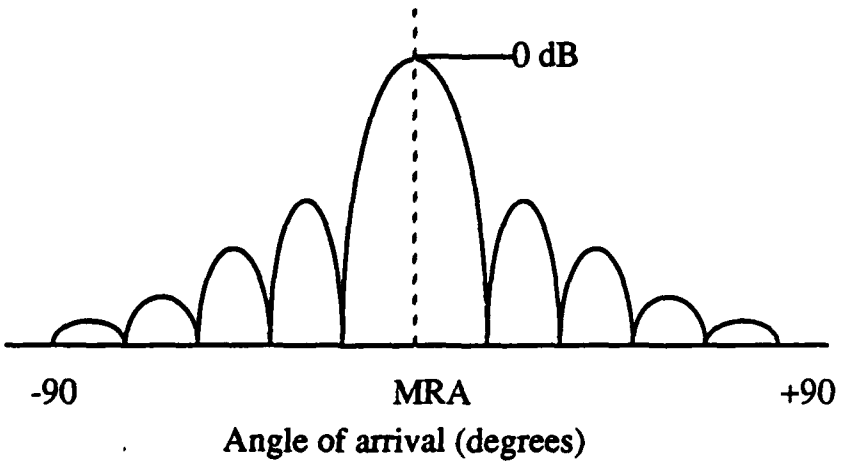

Figure 2.3 Conventional beamformer beampattern.

2.6 Adaptive Beamforming

As in spectral estimation there are several techniques of beamforming that are dependent on the data. These algorithms are known as adaptive beamforming (ABF). Typically the ABF techniques are characterized by high resolution beams and often an optimality criterion. Adaptive beamformers find their origin in the 1960's with the work of people such as Applebaum, Byrn, Griffiths, et al.

The adaptive technique used in this paper is in conjunction with the Minimum Variance Distortionless Response (MVDR) beamformer. This is an optimal technique that minimizes the noise

variance at the output of a beam while constraining the response of the beamformer to a source impinging on the beam's MRA to be distortionless, i.e. to have a frequency response at the MRA with constant magnitude and zero phase. It will be shown that the minimum beam output noise variance condition also satisfies the maximum array gain, maximum beam output SNR and minimum beam output power conditions.

Adaptive beamforming provides an increase in the resolution of a beam over a conventional beamformer under certain conditions. The increased resolution assists in the estimation of the direction of arrival of a signal impinging on the array of sensors.

In order to implement the optimal beamforming algorithm some information about the traveling waves impinging on the array is necessary. The covariance matrix contains that information and if it is not known a priori it must be estimated. The data dependent characteristic of adaptive beamforming is in the estimation of the N-by-N (for an array of N sensors) covariance matrix. The covariance matrix is covered in detail in Section 3.1. In reference [2] Owsley states that the variance of the exponentially averaged covariance matrix estimator is inversely proportional to S-N+1 where S is the number of independent updates made to the estimate and N is the number of sensors (it is assumed that S is greater than N).

The MVDR ABF algorithm requires the inverse of the covariance matrix post multiplied by a known vector. As seen in [2] this requires on the order of N^2 numerical operations utilizing a Cholesky square root factorization of the covariance matrix. A numerical operation is considered to be a complex multiply and add. Comparatively a CBF only requires N numerical operations to compute a single beam output.

The costs of using ABF thus include a noise variance on each beam output due to the uncertainty of the estimated covariance matrix and the increased number of numerical operations required.

2.7 Reduced Dimension Adaptive Beamforming

There have been several studies [1, 2, 3, 4 and 12] concerning methods of reducing the dimension of the adaptive process in ABF, resulting in a reduction in the numerical intensity and possibly the estimation noise variance. Three of the more promising algorithms have been chosen to be discussed here: The subarray preprocessor introduced by Owsley in [2], the beam space preprocessor presented by Gray in [3], and finally the enhanced minimum variance beamformer developed by Owsley in [1] and [10].

The subarray and beam space methods are both characterized by a matrix preprocessor operating on the array sensor data reducing the data vector size and the adaptive dimension from N to M as shown in [4]. An adaptive MVDR beamforming process is

performed on the M dimensional output of the matrix preprocessor. A reduction in the number of numerical operations is achieved because of the reduced dimension of the adaptive process.

The enhanced minimum variance beamformer (EMVDR) uses an estimate of the covariance matrix based on its dominant modes to compute the beamformer weights and delays. Only the D dominant eigenvectors must be estimated as compared to the full covariance matrix where D is expected to be much less than N the full dimension. The computational savings is also evident in the eigenvector estimation algorithm.

The purpose of this thesis is to develop the theory behind the above three reduced dimension adaptive beamforming techniques and compare them to conventional beamforming and to a full array adaptive MVDR beamformer.

CHAPTER 3 - THEORY

3.0 Introduction

This section is intended to describe the models and assumptions used in the development of the beamformers including the introduction of the "steering vector" and the covariance matrix. Conventional beamforming is discussed along with a beamformer's beampattern and beam response. The MVDR algorithm with a matrix preprocessor is developed followed by an in depth discussion of the subarray preprocessor. The beam space preprocessor is presented and finally the enhanced minimum variance beamformer is derived.

The variable notation used throughout the text has the following explanation: scalars are generally lower case non-bold characters, vectors are lower case bold, matrices are upper case bold, and Fourier transforms may be either upper or lower case of the time domain signal depending on the situation.

3.1 Models and Assumptions

As mentioned in Section 2.4 and described in Figure 2.2 the example used to develop the beamformers will be an array of sensors configured in a straight line with equal spacing between each sensor. The sensor is a transducer that converts a physical force into a voltage signal. The voltage signal is then sampled in time. The resulting discrete voltage signal is converted into the frequency domain by the use of an FFT. Figure 3.1 depicts this process. A

vector is formed by taking the same frequency bin (FFT output) from each sensor signal. This is known as the frequency data vector. For wideband processing this must be done for several frequency bins.

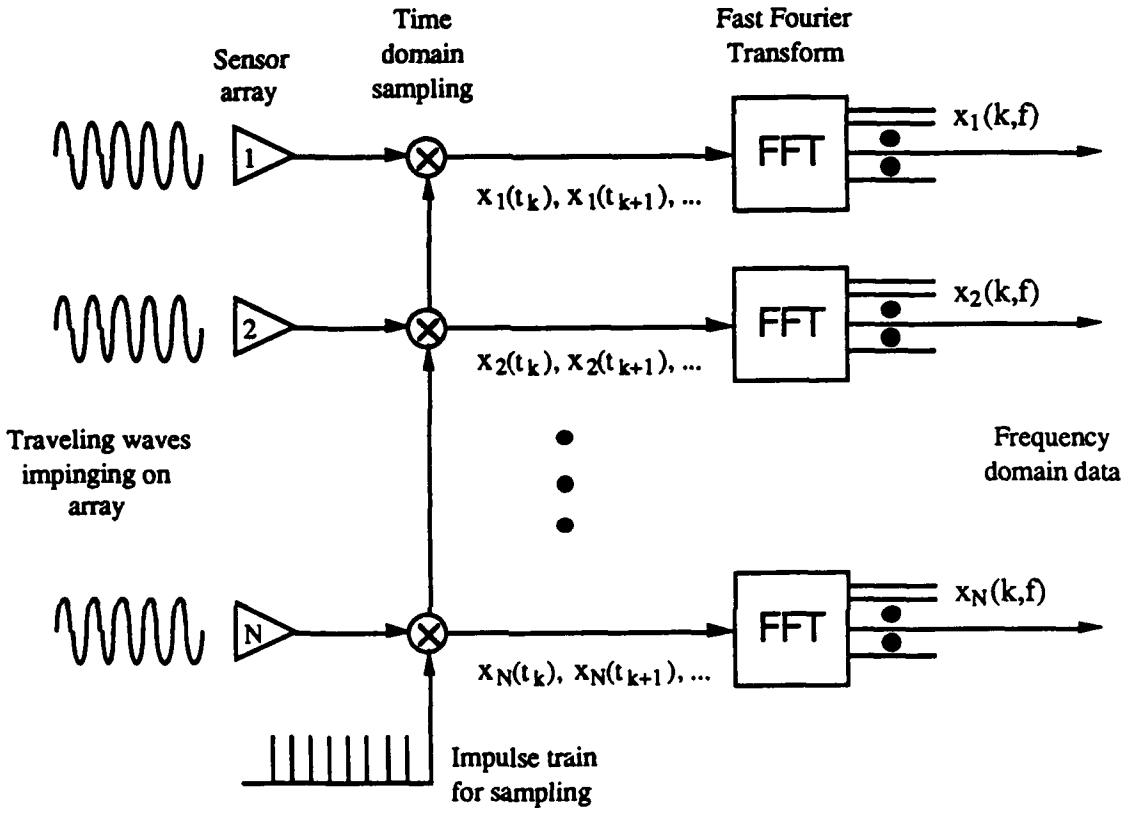

Figure 3.1 Pre-beamformer signal path.

Figure 2.2 illustrates a point source producing waves propagating spherically. It is assumed that all point sources are in the far field. The far field or plane wave assumption is that the length of the array of sensors is small compared to the distance between the source and the array. If this is so the wavefront, as it arrives at the array, is very near to being planar. Figure 3.2 depicts a plane wave impinging on a line array from the angle theta. The

resulting time delay between the first and the i^{th} sensor is seen to be,

$$\tau_i = \frac{d\sin(\theta)(i - 1)}{c}, \qquad 3\text{-}1$$

where c is the speed of of the traveling wave and d the distance between adjacent sensors.

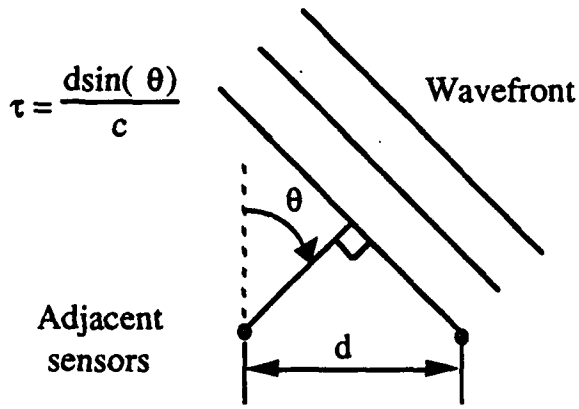

Figure 3.2 Delay between adjacent sensors.

Grouping all of the sensor outputs due to the signal into a vector and incorporating the delays, τ_i, yields,

$$\mathbf{a}(t) = [a(t-\tau_1)\ a(t-\tau_2) \cdots a(t-\tau_N)]^T ,$$

where a(t) is the amplitude of the received waveform at the first or reference sensor and the superscript "T" denotes the transpose operation. Computing the Fourier transform of the time domain data vector yields,

$$\mathbf{a}(f) = \int_{-\infty}^{+\infty} \mathbf{a}(t)\, e^{-j2\pi ft}\, dt$$

$$\mathbf{a}(f) = A(f)\, [\, e^{-j2\pi f\tau_1}\, e^{-j2\pi f\tau_2} \cdots e^{-j2\pi f\tau_N}]^T$$

$$\mathbf{a}(f) = A(f)\, \mathbf{d}(f,\theta) \qquad 3\text{-}2$$

where A(f) is the Fourier transform of a(t). It is assumed that A(f) has zero mean, E[A(f)]=0, and variance $E[A(f)A^*(f)] = S$, where S is frequency dependent.

The vector $\mathbf{d}(f,\theta)$ is dependent on the frequency and the angle of arrival of the plane wave, the array sensor spacing and the speed of the traveling wave. This vector is known as the steering vector and will be seen to play an important role in beamforming. The steering vector is developed here for the simple line array case. More complex array configurations only require that the relative delay between a reference sensor and every other sensor be calculable or measurable.

In reality the sensors receive noise as well as signals from the ambient background and electronic noise from amplifiers and other hardware. This noise is modelled as being uncorrelated from sensor to sensor and additive to the received voltage signal, i.e.

$$\mathbf{x}(f) = \mathbf{a}(f) + \mathbf{n}(f) \qquad 3\text{-}3$$

where $\mathbf{n}(f)$ is the Fourier transform of the received noise. The frequency noise vector is characterized by having a complex zero mean ($E[\mathbf{n}(f)]=\bar{\mathbf{n}}(f)=\mathbf{0}$) and a covariance matrix defined by:

$$\mathbf{Q} = E[(\mathbf{n} - \bar{\mathbf{n}})(\mathbf{n} - \bar{\mathbf{n}})^H] = E[\mathbf{n}\mathbf{n}^H] = \sigma^2 \mathbf{I}_N$$

where the superscript "H" denotes a complex conjugate transpose operation and $\mathbf{I}_N$ is an N-by-N identity matrix. For ease of notation the dependence on frequency will be suppressed for some variables.

The covariance matrix mentioned in Chapters 1 and 2 is the expected value of the outer product of the frequency data vector with itself,

$$\begin{aligned}\mathbf{R} &= E[\mathbf{x}\,\mathbf{x}^H] \\ &= E[(\mathbf{a} + \mathbf{n})(\mathbf{a} + \mathbf{n})^H] \\ &= E[\mathbf{a}\mathbf{a}^H + \mathbf{a}\mathbf{n}^H + \mathbf{n}\mathbf{a}^H + \mathbf{n}\mathbf{n}^H]\end{aligned}$$

Since $\mathbf{a}$ and $\mathbf{n}$ are assumed statistically independent, the expected value of their outer product is zero yielding,

$$\begin{aligned}&= E[\mathbf{a}\mathbf{a}^H + \mathbf{n}\mathbf{n}^H] \\ &= E[A(f)A^*(f)\,\mathbf{d}\mathbf{d}^H] + \sigma^2 \mathbf{I}_N \\ &= E[A(f)A^*(f)]\,\mathbf{d}\mathbf{d}^H + \sigma^2 \mathbf{I}_N \\ &= S\,\mathbf{d}\mathbf{d}^H + \sigma^2 \mathbf{I}_N\,. \end{aligned} \qquad 3\text{-}4$$

Now let there be an arbitrary number of independent or uncorrelated plane wave sources impinging on the array from directions $\theta_1, \theta_2, \cdots \theta_P$ with the associated steering vectors $\mathbf{d}(\theta_1)$, $\mathbf{d}(\theta_2), \cdots \mathbf{d}(\theta_P)$ and source powers (variances) $S_1, S_2, \cdots S_P$. Due to linearity and superposition, the terms resulting from the plane wave sources add to form a covariance matrix of the following form:

$$\begin{aligned}\mathbf{R} &= E[\mathbf{x}\,\mathbf{x}^H] \\ &= S_1\,\mathbf{d}_1\mathbf{d}_1^H + S_2\,\mathbf{d}_2\mathbf{d}_2^H + \cdots + S_P\,\mathbf{d}_P\mathbf{d}_P^H + \sigma^2\,\mathbf{I}_N \\ &= [\mathbf{d}_1\,\mathbf{d}_2 \cdots \mathbf{d}_P]\,\mathbf{S}\,[\mathbf{d}_1\,\mathbf{d}_2 \cdots \mathbf{d}_P]^H + \sigma^2\,\mathbf{I}_N \\ &= \mathbf{D}\,\mathbf{S}\,\mathbf{D}^H + \sigma^2\,\mathbf{I}_N \end{aligned} \qquad 3\text{-}5$$

where $\mathbf{D} = [\mathbf{d}_1\,\mathbf{d}_2 \cdots \mathbf{d}_P]$, and $\mathbf{S} = \mathrm{diag}[S_1\,S_2 \cdots S_P]$.

The covariance matrix, described by the expected value of the outer product of the frequency data vector with itself, is also known as the cross spectral density matrix (CSDM) for a particular frequency.

3.2 Conventional Beamforming

Conventional beamforming is performed with fixed amplitude scalings and phase shifts that correspond to fixed look directions. The spectrum analysis analog is the bandpass FIR filter. The weights applied to the sensors are similar to the impulse response or coefficients of the FIR filter. The beam output is the sum of the

products of the complex sensors weights and the sensor data, i.e. the discrete convolution of the two.

The spectral analysis technique known as the Welch periodogram [9] is performed using the DFT which is simply a bank of FIR bandpass filters. Thus it is seen that the FIR spatial filter (the CBF) applied to the sensor array data is simply estimating the spatial frequency spectrum (at a single spatial frequency) via a Welch periodogram technique. It is convenient to think of a CBF as a spatial bandpass FIR filter. In general several beams are computed to form an estimate of the full spatial spectrum. The spectrum analysis analog is a bank of FIR filters estimating several frequencies (probably implemented as an FFT).

In spectral estimation the resolution achieved by digital Fourier techniques such as periodograms is inversely proportional to the amount of time data that is processed. A similar limit is imposed in conventional beamforming where the amount of data processed is defined by the aperture or extent of the array. The adaptive algorithms, as in spectral estimation, are not restricted by this limit.

The **beampattern** and **beam response** of a beamformer are commonly misunderstood. The beampattern is similar to the transfer function of an FIR filter. It is defined as being the expected response of a beamformer steered to a specific direction (i.e. a fixed set of beamforming weights) due to a single unit variance, zero mean,

plane wave source being swept across all potential angles of arrival [5]. The transfer function of an FIR filter may be measured similarly by sweeping a sine wave across all possible frequencies. The information the beampattern yields is the attenuation that a plane wave signal may expect to receive dependent on its angle of arrival when the beamformer is steered to a fixed angle. As previously mentioned the beampattern provides the "impulse" response or transfer function of the beamformer that yields the output or beam response.

The frequency domain beamformer is represented by the inner product of a beamforming vector of complex weights, $\mathbf{w}(\theta_S)$, with the received frequency data vector,

$$y(\theta_S) = \mathbf{w}(\theta_S)^H \mathbf{x}(f) \ .$$

The output of the beamformer steered to the angle θ_S is $y(\theta_S)$. Note that y is a complex scalar value. The magnitude squared, or instantaneous power, of the beam output is often used as a comparison metric or for display purposes.

Mathematically the beampattern is developed from a fixed set of weights, $\mathbf{w}(\theta_S)$, where θ_S is the angle the beamformer is steered to. The weights may come from any type of beamformer. The expected value of the magnitude squared of the beamformer output is the beampattern,

$$b(\theta_S,\theta) = E[|w(\theta_S)^H x(f,\theta)|^2] \qquad 3\text{-}6$$

where $x(f,\theta)$ represents the frequency domain data vector due to a unit variance, zero mean, plane wave emanating from the angle θ. As seen in Section 3.1 the frequency domain data vector due to a plane wave source is modeled as a random complex scalar multiplied by a steering vector for the array steered to the direction of the source,

$$x(f,\theta) = A(f)d(\theta) ,$$

where the complex multiplier, A(f), has zero mean, $E[A(f)] = 0$, and unit variance $E[|A(f)|^2] = 1$. Now simplifying the beampattern,

$$\begin{aligned} b(\theta_S,\theta) &= E[w(\theta_S)^H x(f,\theta)x(f,\theta)^H w(\theta_S)] \\ &= E[A(f)A^*(f)w(\theta_S)^H d(\theta)d(\theta)^H w(\theta_S)] \\ &= E[A(f)A^*(f)]\ w(\theta_S)^H d(\theta)d(\theta)^H w(\theta_S) \\ &= E[|A(f)|^2]\ |w(\theta_S)^H d(\theta)|^2 \\ &= |w(\theta_S)^H d(\theta)|^2 \end{aligned} \qquad 3\text{-}7$$

The direction of the unit variance, zero mean, plane wave source, θ, is swept through all possible arrival angles (-90 to +90 degrees). The resulting plot of $b(\theta_S,\theta)$ against the source arrival angle, θ, is the beampattern of the beamformer steered to the angle θ_S.

A conventional beamformer delays, scales and sums the sensor outputs. The delays are determined by the direction the beamformer is steered to and as seen in Section 3.1 are a function of the array spacing, speed of the traveling wave and steering angle (for the line array example). The shadings utilized are similar to those used in digital filter design. The uniform and Chebyshev (with 30dB sidelobes) shadings will be utilized here. Figures 3.3 and 3.4 depict the beampattern of a uniformly and Chebyshev shaded conventional beamformer steered to an angle of 30 degrees.

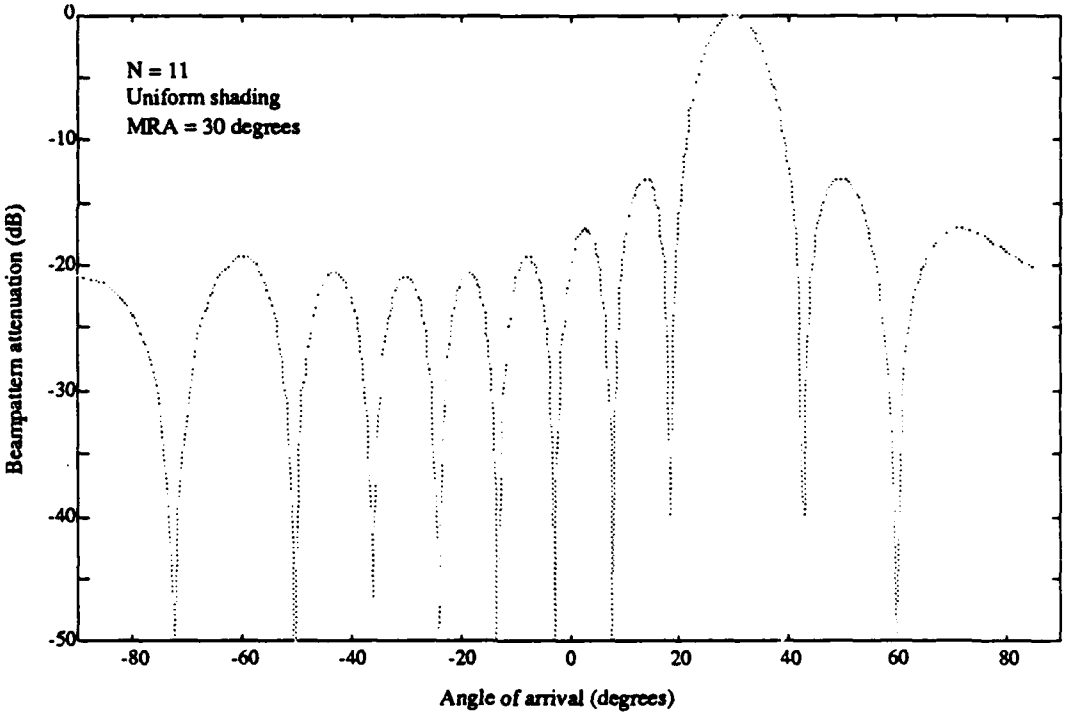

Figure 3.3 Uniform CBF beampattern steered to 30 degrees.

The characteristics of the Chebyshev shading, the constant sidelobe level, lower than that of uniform sensor shading at the expense of mainlobe width, are seen in Figure 3.4.

The beamforming vector for a conventional beamformer, steered to the angle θ_s, as represented by the delays and shadings is

$$\mathbf{w}(\theta_s) = \mathbf{W}\ \mathbf{d}(\theta_s)$$

where $\mathbf{W}$ is a diagonal matrix containing the shadings and $\mathbf{d}(\theta_s)$ is an array steering vector steered to the angle θ_s. The beampattern for a conventional beamformer is thus seen to be

$$b_{CBF}(\theta_s,\theta) = |\mathbf{d}(\theta_s)^H \mathbf{W} \mathbf{d}(\theta)|^2 \qquad 3\text{-}8$$

where $\mathbf{W}$ is real and diagonal.

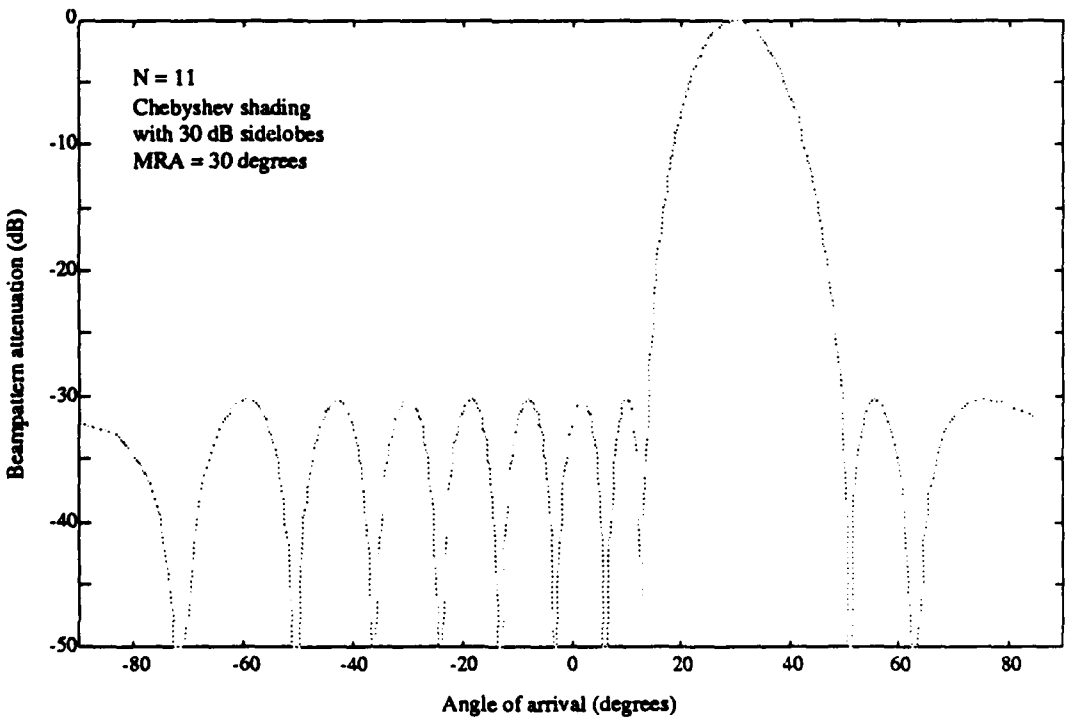

Figure 3.4 Chebyshev CBF beampattern with 30 dB sidelobes steered to 30 degrees.

The beam response of a beamformer is the output power of a fan of beams spanning the potential arrival angles. The spectrum analysis analog is the estimate of the power in several frequency bins. The beam response is computed by forming several beams and taking the magnitude squared of the output. The average or expected response includes the expectation operator as follows,

$$\begin{aligned} r(\theta) &= E[|\mathbf{w}(\theta)^H \mathbf{x}|^2] \\ &= E[\mathbf{w}(\theta)^H \mathbf{x}\mathbf{x}^H \mathbf{w}(\theta)] \\ &= \mathbf{w}(\theta)^H E[\mathbf{x}\mathbf{x}^H]\, \mathbf{w}(\theta) \\ &= \mathbf{w}(\theta)^H \mathbf{R}\, \mathbf{w}(\theta) \end{aligned} \qquad 3\text{-}9$$

where $\mathbf{x}$ is the received frequency data vector, $\mathbf{R}$ is the CSDM defined in Section 3.1, $\mathbf{w}(\theta)$ is the beamforming vector, and θ is the angle to which each beam is steered to and varies from -90 to +90 degrees.

The average beam response provides the response of the beamformer to a particular scenario for the perfectly known CSDM. In practice the CSDM is never known exactly and scenarios are not stationary for long periods of time. The CSDM is therefore estimated using an exponential averager (see [2], [5] and Appendix A). The beam response for each iteration is calculated as the power output of the beamformer,

$$r(\theta) = |\mathbf{w}(\theta)^H \mathbf{x}|^2. \qquad 3\text{-}10$$

Figures 3.5 and 3.6 show average beam responses for a conventional beamformer with uniform and Chebyshev (with 30 dB sidelobes) shading. The scenario is a plane wave source at zero degrees with 0dB variance and at 30 degrees with -3dB variance amidst spatially uncorrelated background noise with a variance of 0dB at a sensor. There are eleven sensors in the array.

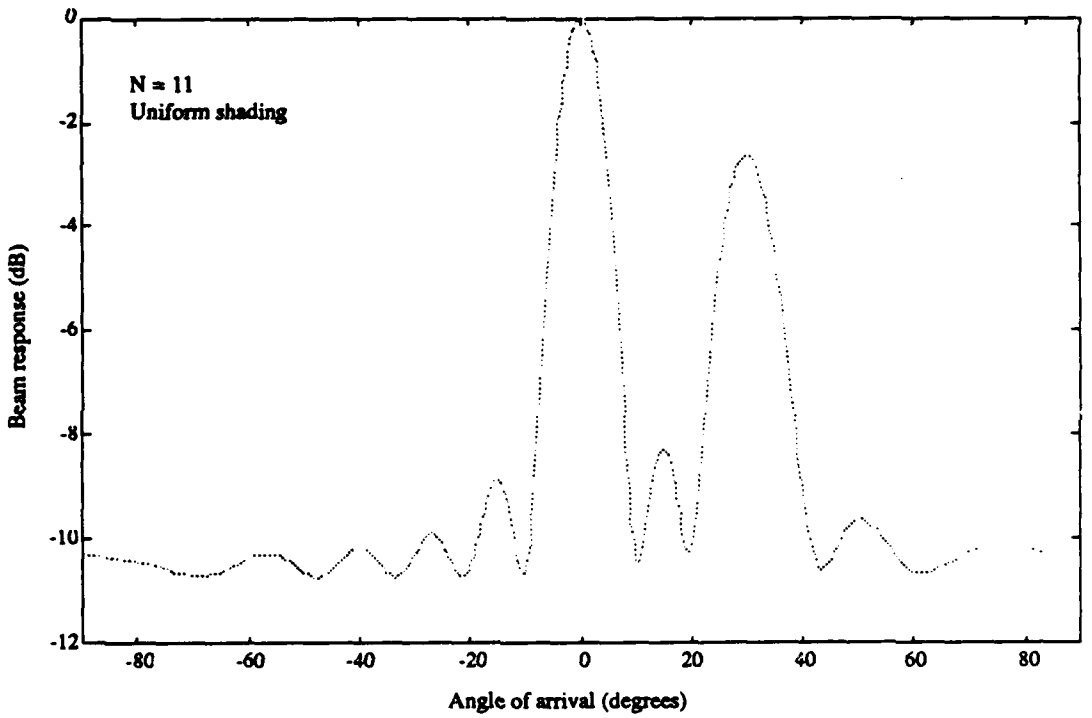

Figure 3.5 CBF beam response with uniform shading.

The average beam response for a conventional beamformer is seen to be,

$$r_{CBF}(\theta) = \mathbf{d}(\theta)^H \mathbf{W}\,\mathbf{R}\,\mathbf{W}\,\mathbf{d}(\theta), \qquad 3\text{-}11$$

by substituting in for the conventional beamforming vector.

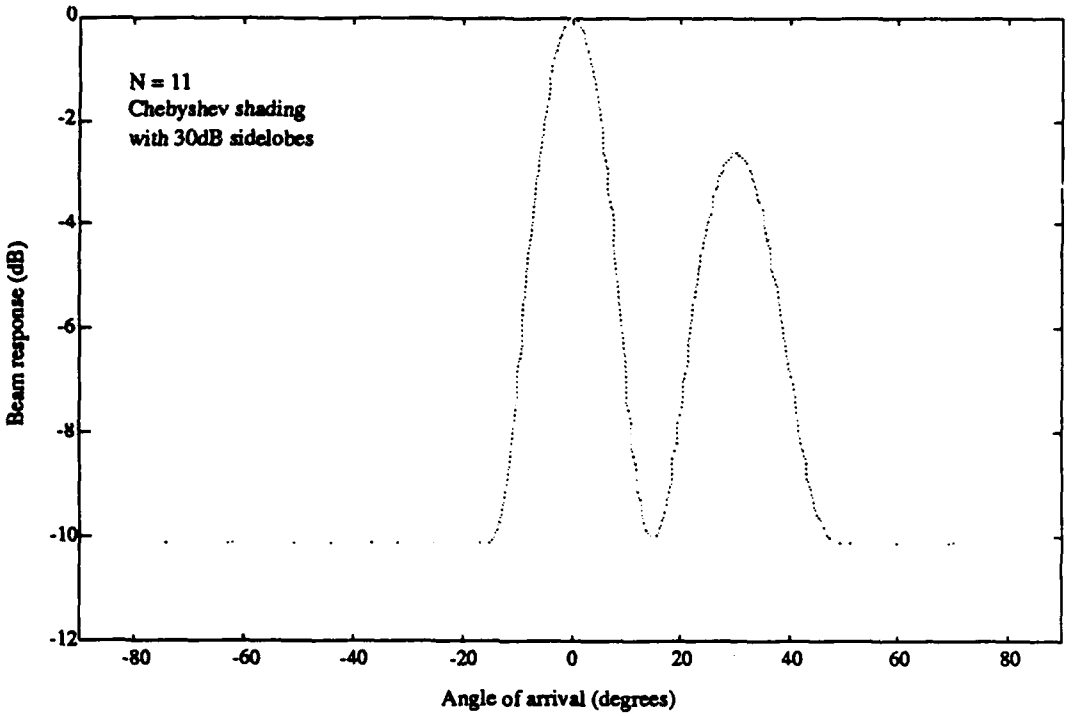

Figure 3.6 CBF beam response with 30 dB Chebyshev shading.

3.3 Matrix Preprocessed MVDR

The subarray and beam space preprocessors may be described in the form of a matrix premultiplier operating on the received frequency data vector. The implementation of this configuration is depicted in Figure 3.7 where the beamformer is separated into a preprocessor and an ABF section. Note that the full array MVDR algorithm is a special case where the matrix preprocessor is an N-by-N identity matrix.

The objective of the matrix preprocessor is to reduce the dimension of the adaptive part of the beamformer from N (the number of sensors) to M. The effect of the reduction lies in the fact that the CSDM that needs to be estimated and inverted is now only

M-by-M thus reducing the total number of numerical operations required to implement the beamformer. Sections 3.3.1 and 3.3.2 cover two particular methods of choosing the matrix used in the preprocessor. As shown in [4] by Owsley and Abraham several types of reduced dimension adaptive beamformers may be implemented in the matrix preprocessor structure.

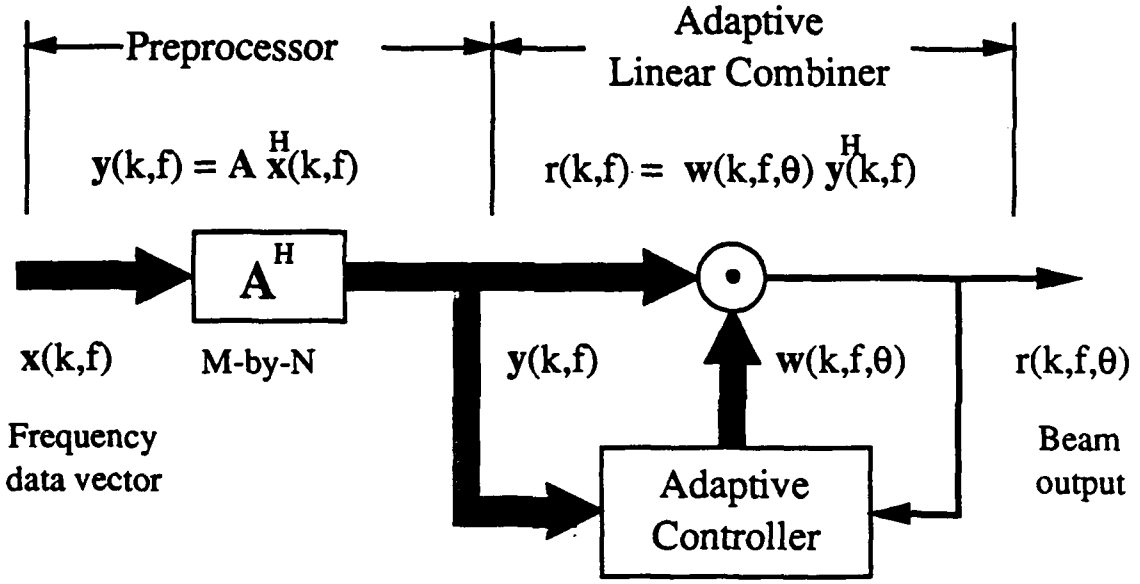

Figure 3.7 Matrix preprocessor - ABF configuration.

The minimum variance distortionless response beamformer may be equivalently derived for the constrained minimization of the variance of a beam output, the maximization of a metric known as the array gain, the maximization of the beam output SNR or the minimization of the total beam output power. Beginning with the maximization of the array gain, the equivalency will be shown. First the frequency data vector is acted on by the preprocessor matrix yielding a reduced dimension data vector,

$$y(\theta_{ps}) = A^H(\theta_{ps})\, x \qquad 3\text{-}12$$

$(M \times 1) \quad (M \times N) \; (N \times 1)$

where θ_{ps} is the presteering angle and $A(\theta_{ps})$ is the preprocessing matrix. Several presteering angles are required to evaluate all the possible arrival angles. The presteering angles are specific to the type of preprocessor matrix used and will be discussed further in Sections 3.3.1 and 3.3.2.

The adaptive beamforming will be performed on the reduced dimension data vector $y(\theta_{ps})$, thus the beam output power or response of a beam steered to angle θ is,

$$r(\theta) = E[|w(\theta)^H y(\theta_{ps})|^2].$$

Note that the beam is pointed to the angle θ and the preprocessor matrix is set to the presteer angle θ_{ps}. For convenience most of the indices denoting these angles will be omitted.

$$\begin{aligned} r(\theta) &= E[w^H y y^H w] \\ &= w^H E[y y^H]\, w \\ &= w^H E[A^H x\, x^H A]\, w \\ &= w^H A^H E[x\, x^H]\, A\, w \\ &= w^H A^H R\, A\, w \end{aligned}$$

In Section 3.1 the CSDM was modeled as the sum of several plane waves and spatially uncorrelated noise,

$$\mathbf{R} = S_1 \mathbf{d}_1\mathbf{d}_1^H + S_2 \mathbf{d}_2\mathbf{d}_2^H + \cdots + S_P \mathbf{d}_P\mathbf{d}_P^H + \sigma^2 \mathbf{I}_N .$$

Let the plane wave denoted by angle θ_1 be from the angle that the beamformer is steered to, θ (i.e. $\theta = \theta_1$). Now an important distinction between signal and interference is made. Any signals impinging on the array from a direction other than the look direction or MRA of the beamformer are considered to be interferences. The uncorrelated background noise is also considered to be interference. Thus the CSDM may be broken up into signal and noise partitions as follows,

$$\mathbf{P} = \mathbf{d}_1\mathbf{d}_1^H = \mathbf{d}\mathbf{d}^H$$
$$S_N \mathbf{Q} = S_2 \mathbf{d}_2\mathbf{d}_2^H + \cdots + S_P \mathbf{d}_P\mathbf{d}_P^H + \sigma^2 \mathbf{I}_N$$

where $\mathbf{P}$ is the signal partition, $\mathbf{Q}$ is the noise partition and S_N is the equivalent variance at a single sensor due to all of the interfering signals. Now the CSDM may be written as,

$$\mathbf{R} = S_1\mathbf{P} + S_N\mathbf{Q}. \qquad 3\text{-}13$$

Substituting this back into the beam response power equation yields

$$r(\theta) = \mathbf{w}^H\mathbf{A}^H (S_1\mathbf{P} + S_N\mathbf{Q})\, \mathbf{A}\,\mathbf{w}$$

$$= S_1 \mathbf{w}^H \mathbf{A}^H \mathbf{P} \mathbf{A} \mathbf{w} + S_N \mathbf{w}^H \mathbf{A}^H \mathbf{Q} \mathbf{A} \mathbf{w} \qquad 3\text{-}14$$

It is desired to maximize the array gain (AG). The array gain is defined by Burdic in [8] as the ratio of the SNR at the output of the beamformer to the SNR at a single sensor.

$$AG = \frac{SNR_{OUT}}{SNR_{IN}} \qquad 3\text{-}15$$

The SNR at a single sensor is simply

$$SNR_{IN} = \frac{S_1}{S_N} . \qquad 3\text{-}16$$

The SNR of the beam response output is seen to be the ratio of the signal and noise partitions of the above equation for the beam response output power.

$$SNR_{OUT} = \frac{S_1 \mathbf{w}^H \mathbf{A}^H \mathbf{P} \mathbf{A} \mathbf{w}}{S_N \mathbf{w}^H \mathbf{A}^H \mathbf{Q} \mathbf{A} \mathbf{w}} . \qquad 3\text{-}17$$

The array gain is then

$$AG = \frac{\mathbf{w}^H \mathbf{A}^H \mathbf{P} \mathbf{A} \mathbf{w}}{\mathbf{w}^H \mathbf{A}^H \mathbf{Q} \mathbf{A} \mathbf{w}} . \qquad 3\text{-}18$$

The constraint applied to the beamformer keeps a source coming from the angle that the beam is pointed to distortionless. This means that the signal must receive no phase change and only a

specified amount of gain. Here the gain is chosen as N, the number of sensors. This is to insure that the ABF array gain matches the CBF array gain. The constraint is written as,

$$\mathbf{w}^H\mathbf{A}^H\mathbf{d} = N. \qquad 3\text{-}19$$

The steering vector **d** and the beamforming vector **w** are pointed to the direction of the beam, and in this case that of the first plane wave source. A cost function, J_1, is generated that includes a Lagrange multiplier, λ, operating on the constraint,

$$J_1 = \frac{\mathbf{w}^H\mathbf{A}^H\mathbf{P}\mathbf{A}\mathbf{w}}{\mathbf{w}^H\mathbf{A}^H\mathbf{Q}\mathbf{A}\mathbf{w}} + 2\lambda(\mathbf{w}^H\mathbf{A}^H\mathbf{d} - N). \qquad 3\text{-}20$$

The beamforming vector, **w**, that maximizes the cost function also maximizes the array gain while preserving the distortionless response constraint. In general the minimization or maximization of the cost function requires that the partial derivative be taken with respect to the beamforming vector, **w**, and its complex conjugate, $\mathbf{w}^*$, and then setting both equal to the zero vector. When the cost function is real it is sufficient to set either partial derivative to the zero vector. The cost function is real here because the function being extremized is real and the constraint is forced to be real. The multiplication of the constraint by 2 doesn't alter the extremization of the cost function for if the constraint is satisfied ($\mathbf{w}^H\mathbf{A}^H\mathbf{d} - N$) will equal zero and the factor 2 provides a simpler algebraic equation than would otherwise have occurred.

The maximization of the beam output SNR condition is easily seen to be the previous equation for the array gain multiplied by the constant sensor level SNR yielding a cost function,

$$J_2 = SNR_{IN} \frac{\mathbf{w}^H\mathbf{A}^H\mathbf{P}\mathbf{A}\mathbf{w}}{\mathbf{w}^H\mathbf{A}^H\mathbf{Q}\mathbf{A}\mathbf{w}} + 2\lambda(\mathbf{w}^H\mathbf{A}^H\mathbf{d} - N). \qquad 3\text{-}21$$

The minimization of the beam output noise variance may be seen by substituting the constraint into the expanded numerator of the equation for the array gain,

$$\begin{aligned} J_3 &= \frac{\mathbf{w}^H\mathbf{A}^H\mathbf{d}\mathbf{d}^H\mathbf{A}\,\mathbf{w}}{\mathbf{w}^H\mathbf{A}^H\mathbf{Q}\mathbf{A}\mathbf{w}} + 2\lambda(\mathbf{w}^H\mathbf{A}^H\mathbf{d} - N) \\ &= \frac{N^2}{\mathbf{w}^H\mathbf{A}^H\mathbf{Q}\mathbf{A}\mathbf{w}} + 2\lambda(\mathbf{w}^H\mathbf{A}^H\mathbf{d} - N)\,. \end{aligned} \qquad 3\text{-}22$$

The minimization of the beam output noise power or variance is equivalent to the maximization of its inverse. The denominator of the above cost function is the power output of the beam due to the noise or interference portion of the signals impinging on the array.

The minimization of the total beam output power may be seen by rewriting the cost function J_3 as a minimization rather than an maximization,

$$J_4 = \mathbf{w}^H\mathbf{A}^H\mathbf{Q}\mathbf{A}\mathbf{w} + 2\lambda(\mathbf{w}^H\mathbf{A}^H\mathbf{d} - N).$$

Now substituting in for the noise partition, $\mathbf{Q}$, and the constraint on the beamforming vector, $\mathbf{w}$,

$$J_4 = \mathbf{w}^H\mathbf{A}^H\mathbf{R}\mathbf{A}\mathbf{w} - \mathbf{w}^H\mathbf{A}^H\mathbf{d}\mathbf{d}^H\mathbf{A}\mathbf{w} + 2\lambda(\mathbf{w}^H\mathbf{A}^H\mathbf{d} - N)$$
$$= \mathbf{w}^H\mathbf{A}^H\mathbf{R}\mathbf{A}\mathbf{w} - N^2 + 2\lambda(\mathbf{w}^H\mathbf{A}^H\mathbf{d} - N). \qquad 3\text{-}23$$

The constants in J_2, J_3 and J_4 due to the application of the constraint or the sensor level SNR do not alter the resulting optimal beamforming vector, $\mathbf{w}$. Note that all cost functions constrain the response of a signal from the direction the beam is pointed in to be distortionless with a gain of N. The functions to be extremized are listed in Table 3.1 for comparison.

Table 3.1 Functions to be extremized as related to various optimal conditions.

Description	Function	Extremum
Array gain	$\frac{\mathbf{w}^H\mathbf{A}^H\mathbf{P}\mathbf{A}\mathbf{w}}{\mathbf{w}^H\mathbf{A}^H\mathbf{Q}\mathbf{A}\mathbf{w}}$	Maximize
Beam output SNR	$SNR_{IN}\frac{\mathbf{w}^H\mathbf{A}^H\mathbf{P}\mathbf{A}\mathbf{w}}{\mathbf{w}^H\mathbf{A}^H\mathbf{Q}\mathbf{A}\mathbf{w}}$	Maximize
Beam output Noise power	$\mathbf{w}^H\mathbf{A}^H\mathbf{Q}\mathbf{A}\mathbf{w}$	Minimize
Beam output power	$\mathbf{w}^H\mathbf{A}^H\mathbf{R}\mathbf{A}\mathbf{w} - N^2$	Minimize

The optimal beamforming vector is most easily found by solving the constrained minimization of the total beam output power in the cost function J_4. The partial derivative of the cost function with respect to the beamforming vector is,

$$\frac{\partial}{\partial \mathbf{w}} J_4 = 2\mathbf{A}^H\mathbf{R}\mathbf{A}\mathbf{w} + 2\lambda\mathbf{A}^H\mathbf{d}$$

Now setting this equal to zero and solving for the beamforming vector, $\mathbf{w}$,

$$\frac{\partial}{\partial \mathbf{w}} J_4 = 0$$

$$\mathbf{w} = -\lambda(\mathbf{A}^H\mathbf{R}\mathbf{A})^{-1}\mathbf{A}^H\mathbf{d} \qquad 3\text{-}24$$

This equation for $\mathbf{w}$ is substituted into the constraint equation which is then solved for the Lagrange multiplier λ,

$$\mathbf{w}^H\mathbf{A}^H\mathbf{d} = N$$

$$-\lambda\, \mathbf{d}^H\mathbf{A}(\mathbf{A}^H\mathbf{R}\mathbf{A})^{-1}\mathbf{A}^H\mathbf{d} = N$$

$$\lambda = \frac{-N}{\mathbf{d}^H\mathbf{A}(\mathbf{A}^H\mathbf{R}\mathbf{A})^{-1}\mathbf{A}^H\mathbf{d}} .$$

Note that $(\mathbf{A}^H\mathbf{R}\mathbf{A})^{-1}$ is complex conjugate symmetric. Substituting this back into the equation for $\mathbf{w}$ thus yields,

$$\mathbf{w} = \frac{N\,(\mathbf{A}^H\mathbf{R}\mathbf{A})^{-1}\mathbf{A}^H\mathbf{d}}{\mathbf{d}^H\mathbf{A}(\mathbf{A}^H\mathbf{R}\mathbf{A})^{-1}\mathbf{A}^H\mathbf{d}}$$

$$= \frac{N\,\mathbf{R}_P^{-1}\mathbf{A}^H\mathbf{d}}{\mathbf{d}^H\mathbf{A}\mathbf{R}_P^{-1}\mathbf{A}^H\mathbf{d}} \qquad 3\text{-}25$$

$$\mathbf{R}_P = \mathbf{A}^H\mathbf{R}\mathbf{A}$$

$$= \mathbf{A}^H E[\mathbf{x}\mathbf{x}^H]\mathbf{A}$$

$$= E[yy^H]$$

where $y = A^H x$ is the reduced dimension frequency data vector and R_P is the reduced dimension CSDM defined as the expected value of the outer product of the reduced dimension data vector with itself.

The reduced dimension CSDM, R_P, may be estimated from the reduced dimension frequency data vector, y. There exist several methods of estimating the CSDM of a frequency data vector [5]. The method used in Section 4.3 for the stochastic analysis of the beamformers is an exponential average of a rank one update of the CSDM [2] & [5]. In particular the Cholesky square root factor of the CSDM is what is updated. This method is covered in detail in [5] and in Appendix A.

The development of the MVDR beamformer is covered in detail in [1] and [5]. The matrix preprocessor development is a simple extension that came from work done for [4].

3.3.1 Subarray Preprocessing

Subarray preprocessing consists of forming several smaller overlapping arrays out of all of the sensors of the full array. The smaller arrays, known as subarrays, are then beamformed using conventional techniques to form several beam outputs. A beam output from each subarray (steered to the same direction) is adaptively combined according to the previous section's development

of the matrix preprocessed MVDR beamformer. The concept of forming subarrays prior to adaptive beamforming is alluded to by Owsley in [2]. Figure 3.8 shows how an array may be partitioned into subarrays, each with a beam pointed to a certain direction.

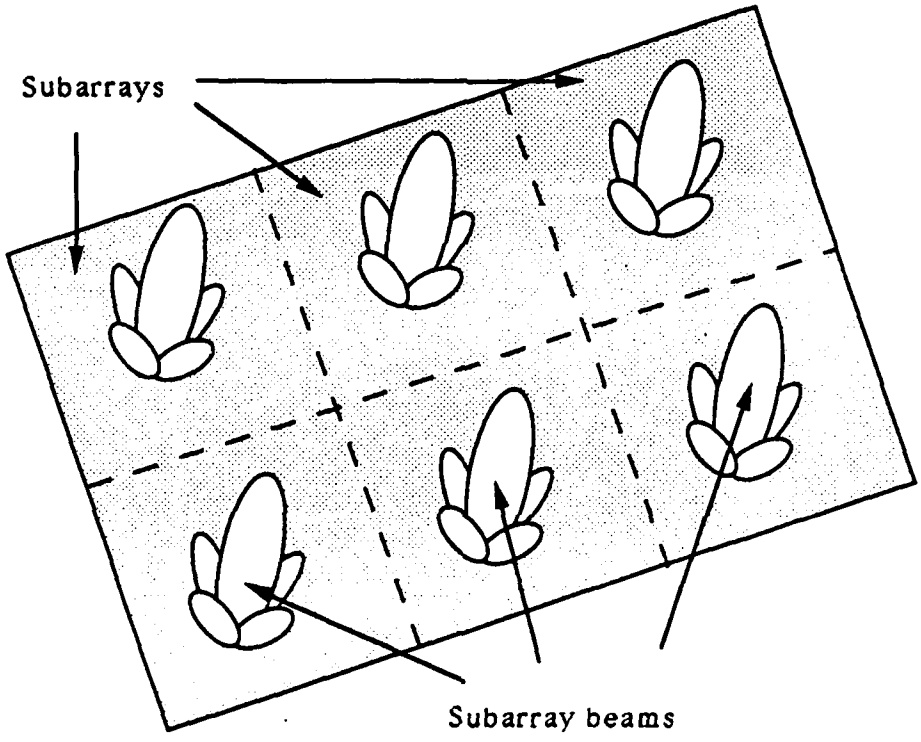

Figure 3.8 Full array partitioned into subarrays.

The preprocessing matrix is comprised of conventional beamforming vectors placed such that they pick off the sensors in each subarray and combine them to form the beam outputs. A typical subarray preprocessor matrix will have the form,

$$\mathbf{A}(\theta_p) = \begin{bmatrix} \mathbf{w}(\theta_p) & \mathbf{0} & & \mathbf{0} \\ & \mathbf{w}(\theta_p) & \cdots & \\ \mathbf{0} & \mathbf{0} & & \mathbf{w}(\theta_p) \end{bmatrix} \qquad 3\text{-}26$$

where $\mathbf{w}(\theta_p)$ is a conventional beamforming vector that is the length of a subarray, θ_p is the direction that the subarray beams are steered to, and $\mathbf{0}$ is a variable dimension vector of zeros.

A particular concern in this method of preprocessing lies in the choice of the subarray size, shading and spacing of the phase centers. The energy field the sensors are immersed in is sampled in discrete locations. This sampling process is similar to the sampling of a time waveform where aliasing is avoided by sampling above the Nyquist sample rate. In time waveforms the signal is filtered prior to the sampling to insure that any energy at frequencies that would alias during the sampling is attenuated as much as possible. Spatial sampling does not have this luxury and hence aliasing may not be avoided.

Throughout the paper the spatial analog of temporal frequency, spatial frequency, has been alluded to as an indication of the angle of arrival of a traveling wave impinging on an array. In order to adequately discuss the aliasing concerns of the subarray parameters more depth in the spatial frequency domain is required. Section 3.3.1.1 covers the required information.

3.3.1.1 Wavenumber Analysis

The spacing of the sensors in an array is chosen such that the highest "spatial frequency", known as wavenumber, that is desired to be evaluated is not aliased at the highest temporal frequency of

concern. The spatial analog to time and period is distance and wavelength,

$$\lambda = \frac{c}{f} , \qquad 3\text{-}27$$

where c is the speed of the propagating wave and f is the frequency of concern. Spatial frequency is measured in wavenumber defined by,

$$k = \frac{2\pi f}{c} \sin(\theta) = \frac{2\pi}{\lambda} \sin(\theta) , \qquad 3\text{-}28$$

for wave propagation along a single axis (i.e. a line array). This is covered by Owsley in [5] for the more general three dimensional wave propagation as well as the single axis case.

The sampling in space, as in time, causes the spectrum of the sampled signal to be the original unsampled spectrum repeated at every multiple of the spatial sampling rate, k_s. The sensors in the array only cover a finite portion of the waves traveling in the medium. This is modeled as an infinite function windowed to a finite aperture. The resulting spectrum is thus the convolution of the transform of the windowing function with the true spectrum. The sampling, windowing and convolution principles can be found in Oppenheim and Schafer [14].

Beamforming the frequency data vector may be viewed as a method of forming an estimate of the spatial spectrum at a single frequency and a particular wavenumber. The frequency and the angle the beam is steered to define the wavenumber. The steering vector used in conventional beamforming is,

$$\begin{aligned}\mathbf{d}(f,\theta) &= [\, e^{-j2\pi f\tau_1}\, e^{-j2\pi f\tau_2} \ldots e^{-j2\pi f\tau_N}]^T \\ &= [\, 1 \;\; e^{-j2\pi f d\sin(\theta)/c} \ldots e^{-j2\pi f d\sin(\theta)(N-1)/c}]^T \\ &= [e^{-j2\pi f d\sin(\theta) i/c}] \qquad i = 0,\ldots,N-1 \\ &= [e^{-jb_i}]\end{aligned}$$

Looking at the exponent only,

$$\begin{aligned}b_i &= 2\pi f d\sin(\theta) i/c \\ &= \frac{2\pi f}{c} \sin(\theta)\, d\, i \\ &= k\, d\, i \end{aligned} \qquad 3\text{-}29$$

The sensor spacing of the array is chosen such that it is no greater than one-half of the wavelength of the highest wavenumber of concern. This is related to the frequency that the array is designed for and the speed of the traveling waves in the medium,

$$d = \frac{\lambda_s}{2} = \frac{c}{2f_s} = \frac{\pi}{k_s}.$$

Thus substituting this back into the above equation for the exponent yields,

$$b_i = \frac{k}{k_s}\pi i .$$

The wavenumbers to be evaluated that will produce unique spatial spectrum estimates are seen to lie on $[-k_s, k_s]$ where,

$$k_s = \frac{2\pi f_s}{c} = \frac{2\pi}{\lambda_s} .$$

This may be shown by evaluating a wavenumber with a greater magnitude than k_s,

$$k' = k + k_s,$$

where k is less than k_s. The exponent b_i is then,

$$b_i = \frac{k'}{k_s}\pi i$$

$$b_i = \frac{k + k_s}{k_s}\pi i$$

$$b_i = \frac{-(k_s - k) + 2k_s}{k_s}\pi i$$

$$= \frac{-(k_s - k)}{k_s}\pi i + 2\pi i .$$

Substituting this back into the steering vector causes the "$2\pi i$" term to go away because it is equivalent to a multiplicative one. The value

of wavenumber that is thus evaulated by using k', greater than k_s, is $-(k_s-k)$ which is within the range $[-k_s, k_s]$.

The less than half wavelength spatial sampling may be related to spectral analysis where the time sampling occurs every $\frac{T}{2}$ seconds or less. The unique frequencies are evaluated over $[-f_s, f_s]$, where $f_s \geq \frac{2}{T}$. In this case the Nyquist sampling frequency, or the frequency interval at which the repeated spectra occur is $f_N = 2f_s$.

Figure 3.9 shows the wavenumber - frequency spectrum and the repeated spectra at multiples of the spatial Nyquist sampling rate, $2k_s$. Note that for a fixed travelling wave speed, c, all the spatial energy falls within the shaded region where the boundaries indicate a wave impinging on the array at +90 or -90 degrees from broadside.

The beamforming process estimates the wavenumber spectrum inside of the shaded region seen in Figure 3.9 at a single frequency. The angles the beams are steered to correspond to particular wavenumbers. Wavenumber is related linearly to frequency as seen in the equation relating the two for a fixed angle of arrival.

3.3.1.2 Subarrays

The conventional beamforming of the subarrays may be thought of as applying a wavenumber bandpass finite impulse

response (FIR) filter to the wavenumber spectrum. The output spectrum is bandlimited in wavenumber and may be spatially undersampled. The undersampling is performed by spacing the

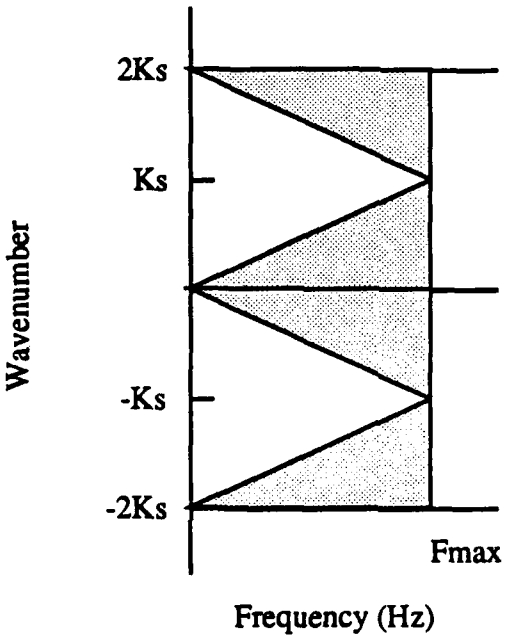

Figure 3.9 Wavenumber spectrum.

phase centers of the subarrays several sensors apart. This is equivalent to convolving the full array frequency domain data vector with the subarray conventional beamforming vector (the impulse response of the FIR filter) and then undersampling the convolved output. The transfer function or beampattern of a subarray is shown on the wavenumber plot at the design frequency of the array in Figure 3.10.

The true spectrum of the energy impinging on the array is thus passed through the filter defined by the subarray conventional

beamforming vector. The filter applies an amplitude and linear phase change to the spectrum. Several wavenumbers centered about the presteer direction (the MRA of the subarray beam) are evaluated. If a signal has a wavenumber that is not on the MRA of the subarray beam it will be attenuated slightly. The wavenumber

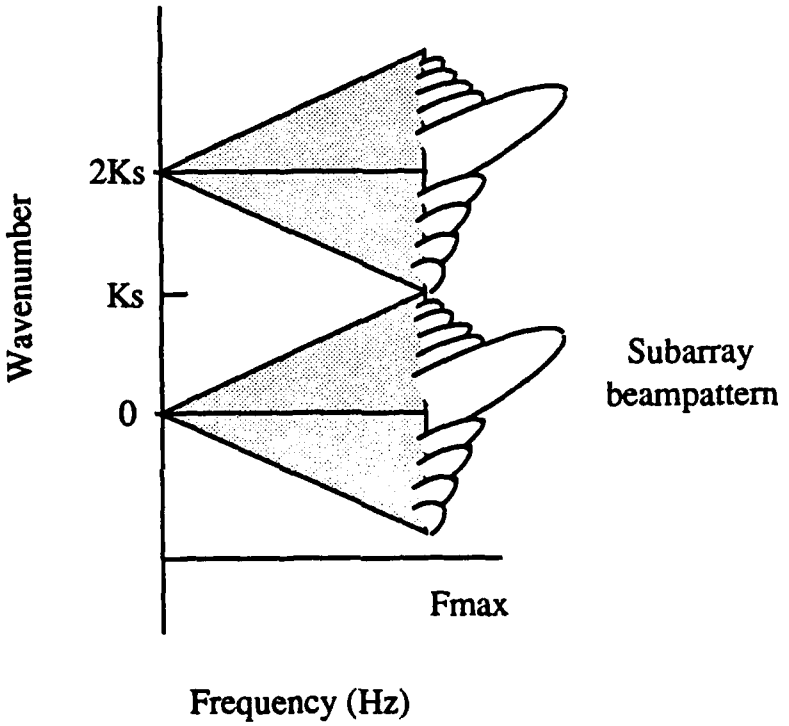

Figure 3.10 Beampattern applied to wavenumber spectrum.

that are evaluated are in the mainlobe of the subarray beampattern and receive a limited amount of attenuation. It is desired to avoid altering the signals impinging on the array significantly. This requires that several adjacent bands of wavenumber be filtered (i.e. several subarray beams or presteer directions) and processed such that the total wavenumber spectrum of concern is evaluated with an

acceptable amount of degradation. The attenuation due to the subarray beamforming is known as scalloping loss.

The undersampling of the spatial spectrum causes the aliasing previously mentioned. The repeated spectra of the wavenumber spectrum is shifted down into the original spectra. This occurs because the new spatial sampling frequency is less than the old one due to the greater separation of the data samples (phase center of the subarrays). Figure 3.11 shows how the subarray beampattern of the repeated spectra is aliased down into the primary spectra on the wavenumber plot. Figure 3.12 shows two adjacent spectra beampatterns and their exact overlap. Note that this occurs for all adjacent pairs of the repeated spectra.

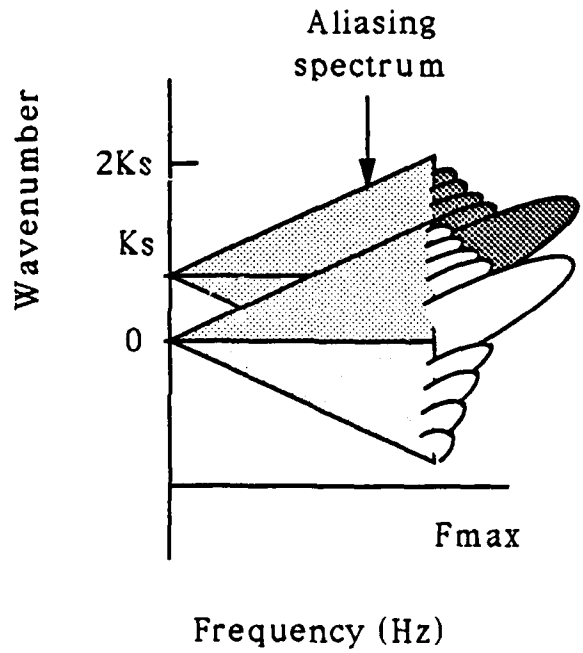

Figure 3.11 Beampattern aliasing with spectrum.

The dimension of the adaptive beamforming performed on the subarray beam outputs is desired to be small as stated in the first two chapters in order to reduce the numerical intensity of the algorithm estimating the inverse of the CSDM. This is in turn reflected into a desire for as few subarrays as possible that will span the full array aperture. This calls for large spacings between subarrays which translates into a very small spatial sampling frequency. This in turn means that it is desired to have the repeated spectra aliased down as far as possible into each adjacent spectra.

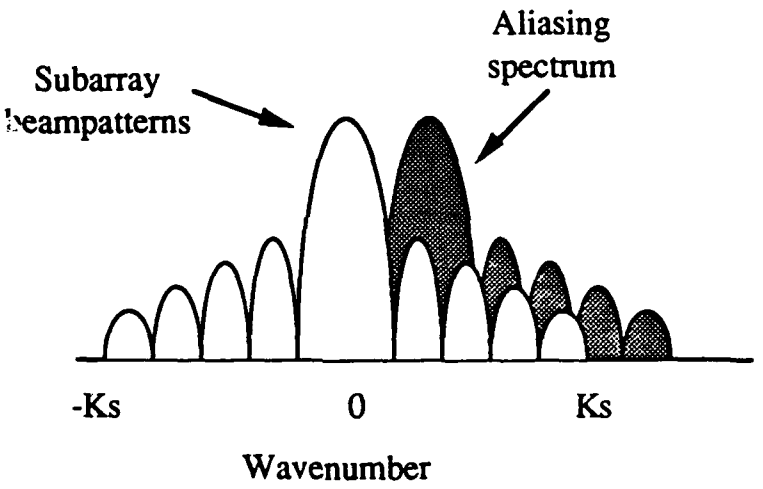

Figure 3.12 Beampattern aliasing.

The high aliasing is **not** desired because it corrupts the estimate of the wavenumber spectrum, the beam output. The compromise between the two conflicting desires was suggested by Dr. Norman Owsley of the Naval Underwater Systems Center (NUSC) to be to allow the aliased spectrum to enter an adjacent one such that

the two mainlobes overlap at the level of the first sidelobe. This condition may be seen in Figure 3.12.

The question arises as to how to determine what subarray sizes, spacings and shadings meet the above aliasing criteria. Due to the discrete sensor location sampling of the spatial field it is required that there be an integer number of sensors between the phase centers of adjacent subarrays. In order that all available data be used it is also required that the subarrays utilize the full aperture of the array, i.e. that the first and last sensors are included respectively in the first and last subarrays.

Figure 3.13 depicts the integer number of sensor spacing of the subarray phase centers and the utilization of the full aperture resulting in the following equation,

$$M = \frac{N-N_S}{N_a} + 1 , \qquad 3\text{-}30$$

where M is the number of subarrays, N_S is the number of sensors per subarray, and N_a is the number of sensors between the phase centers of two adjacent subarrays. Note that M, N, N_S, and N_a must be integers. The number of sensors in the full array, N, is given. For a particular window function used to shade the subarrays the spacing of the subarrays, N_a, for a particular subarray size, N_S, must be tested to see if it is an integer. If it is then the number of subarrays required to span the entire aperture of the array, M, is tested to see

if it is an integer. The resulting valid combinations will satisfy the constraints and conditions previously described.

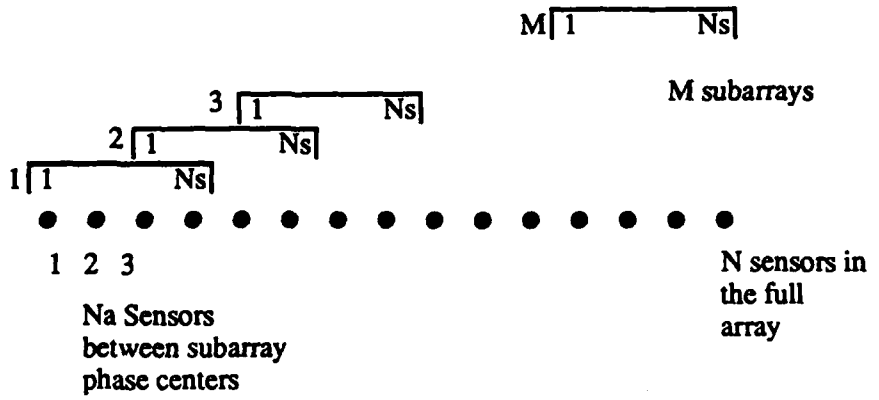

Figure 3.13 Subarray spacing example.

Looking at the exponent of the conventional beamforming vector used to estimate the wavenumber spectrum, as done in Section 3.3.1.1, but evaluating it at the spatial frequency k_s with half wavelength sensor spacing ($d = \lambda_s/2$) yields,

$$b_i(k_s) = k_s \frac{\lambda_s}{2} i \qquad i = 0,\ldots,N-1$$
$$= \frac{k_s}{N_a} \frac{N_a \lambda_s}{2} i$$
$$= k_u \frac{\lambda_u}{2} i$$

where the new spatial sampling period is seen to be $\lambda_u = N_a\lambda_s/2$ and the corresponding sampling wavenumber rate is $k_u = k_s/N_a$. As seen in Figure 3.12 the new sampling rate, k_u, is exactly two times the point at which the two beampatterns overlap in the mainlobe.

The test for the validity of a particular subarray size and shading will be the condition that the ratio of the original wavenumber sample rate to the new sample rate is an integer,

$$N_a = \frac{k_s}{k_u} = \text{INTEGER.} \qquad 3\text{-}31$$

The ratio may be determined by computing the beampattern and finding the wavenumber in the mainlobe that is at the same level as that of the first sidelobe. From this the new wavenumber sampling rate may be determined and the subarray spacing determined.

The beampattern must also be evaluated to find the wavenumber that is at the limit of the allowable scalloping loss. Once this is determined the number of required subarray beams and their particular presteering directions may be determined. Figure 3.14 shows the mainlobe of the subarray beampattern and the region that will be evaluated where the scalloping loss is acceptable, $[-k_{sl}, k_{sl}]$.

The corresponding wavenumber that will be evaluated on each subarray beam will be less than the band shown such that there are an integer number of beams that span the full wavenumber space as shown in Figure 3.15.

The constraint is seen to be in the form of,

$$L_s = \frac{k_s}{k_e} = \text{INTEGER}. \qquad 3\text{-}32$$

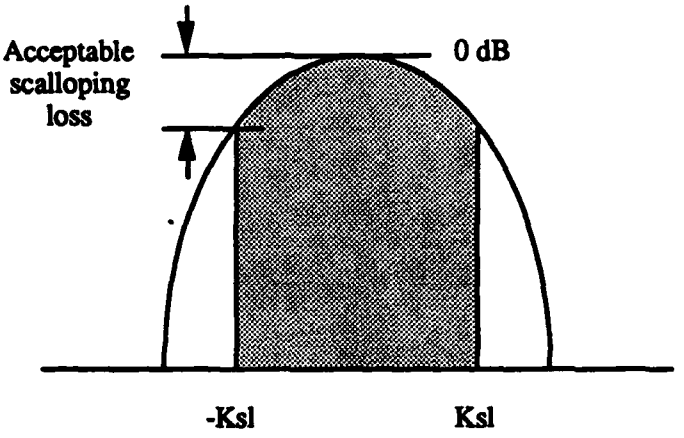

Figure 3.14 Scalloping loss limit on mainlobe of beampattern.

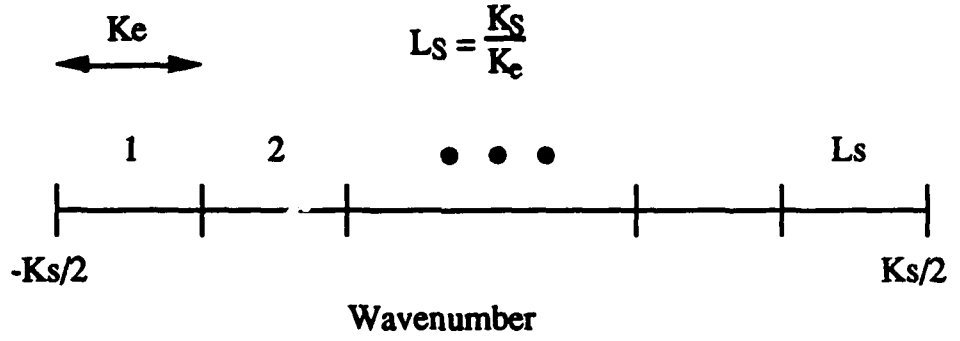

Figure 3.15 Spacing of subarray beams in wavenumber.

The band of wavenumber (k_e wide) that is evaluated for each subarray beam steering direction does not have to terminate as shown in Figure 3.14 where the scalloping loss reaches the maximum allowable. It is desired to have the same width of wavenumber evaluated for all the subarray beam presteer directions and to have the directions be equally spaced in wavenumber.

The algorithm described in Appendix C was used to determine the valid subarray sizes for the beampattern and beam response evaluations of Chapter 4.

Subarray preprocessing is similar to a vernier frequency estimator discussed by Nuttall in [15]. For the subarray beamformer the second or vernier stage of processing is an adaptive spatial spectrum estimator instead of a conventional Fourier method.

3.3.2 Beam Space Preprocessing

Beam space preprocessing was first introduced by Gray in [3]. It is also known as adaptive beam interpolation (ABI). The sensor data is first converted into N (the number of sensors) conventional beam outputs performed using uniform array shading. The MRA's of the N conventional beams are equally spaced in wavenumber. This insures that for half wavelength sensor spacing the interpolation beams are orthogonal ($\mathbf{d}_i^H \mathbf{d}_j = \delta_{ij}$).

Several adjacent beams are then used to interpolate in high resolution the area at the center of the fan of beams. The interpolation is performed with a distortionless response constraint as was developed in Section 3.3.1. The fan of beams "wraps around" when the angles of +90 or -90 degrees from broadside are reached. This is allowed because of the repeated spectra generated in the spatial sampling process as discussed in Section 3.3.1.1.

The mathematical development of the beam space algorithm is covered by Gray in [3]. Reference [4] shows how the beam space algorithm may be implemented in the form of a matrix preprocessor. The preprocessor matrix operating on the array sensor data is formed from the steering vectors that generate the conventional beams. The dimension of the reduced ABF process is equal to the number of beams used in the interpolation. The number of presteer directions is equal to the total number of conventional beams utilized in the interpolation process which is equal to N, the number of sensors.

A simpler but more specific implementation of the beam space preprocessor could take the form of first the computation of the N conventional beams and storage of the complex beam outputs. The beam outputs used for the adaptive algorithm from each presteer direction may then be picked at will. The computational savings of this implementation over the matrix preprocessing is realized by not having to recompute conventional beam outputs for new presteer directions.

This brings to bear a convenient trait of the beam space preprocessor, being that access to the element level data is not required. If the output of a conventional beamformer is the only data available a high resolution beam response estimation may still be performed.

3.4 Enhanced Minimum Variance Beamforming

In [1 & 10] Owsley introduces the enhanced minimum variance beamformer (EMVDR). At low interference to noise ratios the MVDR adaptive beamformer performs the same as the conventional beamformer. This can be seen from the array gain comparison shown in Section 4.1 and [4]. Thus the ABF achieves most of its gain against the stronger interferers impinging on the array. Owsley suggests that the CSDM be approximated by the components due to the stronger, or dominant, signals. This is performed by separating the frequency data vector information into a dominant signal subspace and a complementary space containing all other signals. The dominant signal subspace is then scaled or enhanced.

Mathematically the development of the EMVDR beamformer comes from the eigenvalue-eigenvector decomposition of the CSDM. Recall from Section 3.1 the CSDM was represented as,

$$\mathbf{R} = \mathbf{D}\,\mathbf{S}\,\mathbf{D}^{H} + \sigma^2\,\mathbf{I}_N\,. \qquad 3\text{-}5$$

The eigen-decomposition may be represented as,

$$\mathbf{R} = \mathbf{M}\Lambda\mathbf{M}^{H}, \qquad 3\text{-}33$$

where the columns of $\mathbf{M}$ are the orthonormal eigenvectors of $\mathbf{R}$ and Λ is a diagonal matrix of the eigenvalues. As seen in Brogan [6] and

derived from the definition of **R**, the following are some of the properties of the eigenvalues and eigenvectors of **R**,

- The eigenvectors of $\mathbf{D}\,\mathbf{S}\,\mathbf{D}^H$ are also eigenvectors of **R**
- If ψ_i are the eigenvalues of $\mathbf{D}\,\mathbf{S}\,\mathbf{D}^H$ then
  $\lambda_i = \psi_i + \sigma^2$ are the eigenvalues of **R**
- $\mathbf{D}\,\mathbf{S}\,\mathbf{D}^H$ is positive semidefinite so that $\psi_i \geq 0$ for all i
- Since $\mathbf{R} = \mathbf{R}^H$, then $\mathbf{M}\Lambda\mathbf{M}^H = \mathbf{M}\Lambda^H\mathbf{M}^H$, or $\Lambda = \Lambda^H$, meaning that the eigenvalues of **R** are real
- If σ^2 and the source powers in the diagonal matrix **S** are greater than zero then the eigenvalues of **R** are all positive and greater than zero (**R** is positive definite)

Taking the D dominant eigenvalues and associated eigenvectors and separating them as follows,

$$\mathbf{E} = \mathbf{N}\Psi\mathbf{N}^H \qquad 3\text{-}34$$

where **N** is an N-by-D matrix whose columns are the D eigenvectors of $\mathbf{D}\,\mathbf{S}\,\mathbf{D}^H$ corresponding to the D largest eigenvalues, ψ_i, and Ψ is a diagonal matrix of those eigenvalues.

The exact number of sources does not need to be known, only the dominant or very strong ones. Many high resolution source subspace beamformers, direction finders or spectrum estimators require that the **exact** number of sources be known in order for the algorithm to work. There has been much work in the area of estimating the number of sources impinging on an array or the

number of sinusoids present in a time domain signal. Most of the work requires that the background noise be spatially uncorrelated. Angularly extended noise generates eigenvalues that may be confused with the plane wave source eigenvalues. Thus in the presence of angularly extended noise the eigenvalue methods of estimating the number of sources fall apart. The EMVDR algorithm in contrast only requires the number of strong plane wave sources. It is expected that this problem will not be as difficult as requiring knowledge of the exact number of sources.

Once the dominant source subspace, $\mathbf{E}$, is determined an estimated and enhanced CSDM is formed as,

$$\begin{aligned}\hat{\mathbf{R}}(e) &= e\mathbf{E} + \sigma^2\mathbf{I}_N \\ &= e\mathbf{N}\Psi\mathbf{N}^H + \sigma^2\mathbf{I}_N\end{aligned} \qquad 3\text{-}35$$

where e is the enhancement factor.

The estimated CSDM is used in an MVDR algorithm operating on the full array frequency data vector. The beamforming vector equation is found by setting the preprocessor matrix equal to an N-by-N identity matrix in the MVDR development of Section 3.3.1 yielding,

$$\mathbf{w} = \frac{\mathbf{N}\mathbf{R}^{-1}\mathbf{d}}{\mathbf{d}^H\mathbf{R}^{-1}\mathbf{d}}.$$

Replacing $\mathbf{R}^{-1}$ with the approximated CSDM, $\hat{\mathbf{R}}(e)^{-1}$, the beamforming vector becomes,

$$\mathbf{w} = \frac{N\hat{\mathbf{R}}(e)^{-1}\mathbf{d}}{\mathbf{d}^H\hat{\mathbf{R}}(e)^{-1}\mathbf{d}}. \qquad 3\text{-}36$$

Note that the inverse of the CSDM is required and may be found by using the matrix inversion lemma from Brogan [6],

$$(\mathbf{UAV}^H + \mathbf{B})^{-1} = \mathbf{B}^{-1} - \mathbf{B}^{-1}\mathbf{U}(\mathbf{V}^H\mathbf{B}^{-1}\mathbf{U} + \mathbf{A}^{-1})^{-1}\mathbf{V}^H\mathbf{B}^{-1},$$

as follows,

$$\begin{aligned}\hat{\mathbf{R}}(e)^{-1} &= (eN\Psi N^H + \sigma^2 I_N)^{-1} \\ &= \frac{1}{\sigma^2}[I_N - N(I_D + \frac{\sigma^2}{e}\Psi^{-1})^{-1}N^H] \\ &= \frac{1}{\sigma^2}[I_N - N\,B(e)\,N^H]\end{aligned}$$

where $B(e) = (I_D + \frac{\sigma^2}{e}\Psi^{-1})^{-1}$

$$= \text{diag}(\beta_i)$$

if $\beta_i = \frac{1}{1+\sigma^2/(e\psi_i)}$ $\quad i=1,...,D.$

Now post multiplying the inverse CSDM by the steering vector $\mathbf{d}$,

$$\hat{\mathbf{R}}(e)^{-1}\,\mathbf{d} = \frac{1}{\sigma^2}[I_N - N\,B(e)\,N^H]\,\mathbf{d}$$

$$= \frac{1}{\sigma^2}[\mathbf{d} - \mathbf{N}\,\mathbf{B}(e)\,\mathbf{N}^H\mathbf{d}]$$

$$= \frac{1}{\sigma^2}\left[\mathbf{d} - \sum_{i=1}^{D}\beta_i \mathbf{n}_i\mathbf{n}_i^H\mathbf{d}\right] \qquad 3\text{-}37$$

where $\mathbf{N} = [\mathbf{n}_1\ \mathbf{n}_2 \cdots \mathbf{n}_D]$ are the dominant eigenvectors. Placing this back into the equation for the beamforming vector,

$$\mathbf{w} = \frac{\mathbf{N}\left[\mathbf{d} - \sum_{i=1}^{D}\beta_i \mathbf{n}_i\mathbf{n}_i^H\mathbf{d}\right]}{\mathbf{N} - \sum_{i=1}^{D}\beta_i |\mathbf{d}^H\mathbf{n}_i|^2}. \qquad 3\text{-}38$$

This form of the beamforming vector is very revealing in that it shows how a conventional beam is formed with the steering vector, $\mathbf{d}$. Any interferences, defined by the projection of $\mathbf{d}$ onto the dominant eigenvectors $\mathbf{n}_i$, are then removed by steering nulls toward the sources contributing to the information in the dominant eigenvectors.

A considerable advantage of the EMVDR technique is that it requires very few numerical operations for implementation. Kaveh and Yang introduced a very fast algorithm for the estimation of the eigenvalues and eigenvectors of the source or noise subspaces in [7]. The particular algorithm used is covered in Appendix B.

CHAPTER 4 - COMPARISON

4.0 Introduction

This section will compare the reduced adaptive dimension beamformers with conventional and full array adaptive beamformers. The metrics used for comparison are the array gain improvement (AGI) for a single source, single interference and uncorrelated background noise case, the beampatterns, beam responses, and the numerical computation intensities associated with the realization of the beamformers.

4.1 Array Gain Improvement

For the case of a single plane wave source and a single plane wave or point interference (PIN) with spatially uncorrelated background noise the array gain for the adaptive beamformers may be found analytically. The CSDM for the above case according to the models discussed in Section 3.1 is,

$$\mathbf{R} = S_1\mathbf{d}_1\mathbf{d}_1^H + S_2\mathbf{d}_2\mathbf{d}_2^H + \sigma^2\mathbf{I}_N\,, \qquad 4\text{-}1$$

where S_1 and S_2 are respectively the source and interference powers, $\mathbf{d}_1$ and $\mathbf{d}_2$ are their associated steering vectors, and σ^2 is the uncorrelated noise power.

The array gain (AG), as described in Section 3.3, is the ratio of the SNR at the output of the beamformer to the SNR at a single sensor. The single sensor or beamformer input SNR is seen to be,

$$SNR_{IN} = \frac{S_1}{S_2 + \sigma^2} . \qquad 4\text{-}2$$

The beamformer output power (beam response) from Section 3.2 is,

$$r(\theta) = \mathbf{w}(\theta)^H \mathbf{R}\, \mathbf{w}(\theta) .$$

Inserting the above definition for the CSDM for the single source, single interference and uncorrelated background noise case and dropping the dependence on the angle θ,

$$\begin{aligned} r &= \mathbf{w}^H(S_1\mathbf{d}_1\mathbf{d}_1^H + S_2\mathbf{d}_2\mathbf{d}_2^H + \sigma^2\mathbf{I}_N)\mathbf{w} \\ &= S_1\mathbf{w}^H\mathbf{d}_1\mathbf{d}_1^H\mathbf{w} + S_2\mathbf{w}^H\mathbf{d}_2\mathbf{d}_2^H\mathbf{w} + \sigma^2\mathbf{w}^H\mathbf{I}_N\mathbf{w} \\ &= S_1\mathbf{w}^H\mathbf{d}_1\mathbf{d}_1^H\mathbf{w} + S_2\mathbf{w}^H\mathbf{d}_2\mathbf{d}_2^H\mathbf{w} + \sigma^2\mathbf{w}^H\mathbf{w} \\ &= S_1|\mathbf{w}^H\mathbf{d}_1|^2 + S_2|\mathbf{w}^H\mathbf{d}_2|^2 + \sigma^2\mathbf{w}^H\mathbf{w} \end{aligned}$$

The beamformer output SNR is thus seen to be,

$$SNR_{OUT} = \frac{S_1|\mathbf{w}^H\mathbf{d}_1|^2}{S_2|\mathbf{w}^H\mathbf{d}_2|^2 + \sigma^2\mathbf{w}^H\mathbf{w}} . \qquad 4\text{-}3$$

The array gain is then,

$$AG = \frac{(S_2 + \sigma^2)|\mathbf{w}^H\mathbf{d}_1|^2}{S_2|\mathbf{w}^H\mathbf{d}_2|^2 + \sigma^2\mathbf{w}^H\mathbf{w}}$$

$$= \frac{(r + N)|\mathbf{w}^H\mathbf{d}_1|^2}{r|\mathbf{w}^H\mathbf{d}_2|^2 + N\mathbf{w}^H\mathbf{w}}, \qquad 4\text{-}4$$

where r is defined as the ratio of the interference power to the noise power at the output of a conventional beamformer,

$$r = \frac{S_2}{\sigma^2/N} = \frac{NS_2}{\sigma^2}. \qquad 4\text{-}5$$

The array gain improvement, described by Owsley in [4] & [10], is defined as the ratio between the array gain for a particular beamformer and the array gain for a conventional beamformer with uniform shading. The beamforming filter vector, $\mathbf{w}$, for the uniformly shaded conventional beamformer is simply the steering vector $\mathbf{d}$. This beamformer is steered to look at the source of concern, thus $\mathbf{w} = \mathbf{d}_1$. The array gain is then seen to be,

$$AG_{CBF} = \frac{r + N}{1 + rL}, \qquad 4\text{-}6$$

where the following simplifications were applied,

$$\mathbf{d}_i^H\mathbf{d}_i = N$$

$$\mathbf{d}_1^H\mathbf{d}_2 = N\alpha$$

$$|\mathbf{d}_1^H \mathbf{d}_2|^2 = N^2 \alpha\alpha^* \equiv N^2 L,$$

α is in general complex and $0 \leq L \leq 1$.

Note that if there is no interference ($S_2 = r = 0$) the array gain for the conventional beamformer is equal to N. An alternate form of the array gain may be found by manipulating the equation into the form of a constant, N, plus a second term dependent on the interference to noise ratio r,

$$AG_{CBF} = N + \frac{r(1 - NL)}{1 + rL}. \qquad 4\text{-}7$$

This form reveals how the array gain is affected by the interference to noise ratio, r.

The array gain for each of the adaptive beamformers may be found by inserting their beamforming vectors into the above generic AG equation. The AGI is then found by forming the ratio between the adaptive beamformer array gain and the array gain for a conventional beamformer,

$$AGI = \frac{AG_{ABF}}{AG_{CBF}}. \qquad 4\text{-}8$$

An exorbitant amount of algebra is required to place the equations into forms that are meaningful. Some of the results are

seen in [4] and encapsulated in Table 4.1. The EMVDR beamformer AGI was derived allowing for a variable enhancement factor. The parameters associated with the AGI equations are as follows,

Beam space:

$\underline{M}$ = Number of interpolation beams

$\overline{L}$ = Average sidelobe level of interference in M beams

$E = M\overline{L}$

Subarrays:

L = Normalized interference level in full array

$\underline{L_s}$ = Normalized interference level in subarray

$\overline{L}_s$ = Aliased subarray center response

EMVDR:

P = Signal to interference ratio = S_1/S_2

$$\gamma = \frac{2P}{[1 - P] + \sqrt{[1 - P]^2 + 4PL}}$$

e = Dominant source subspace enhancement factor

$r = \frac{NS_2}{\sigma}$ = interference to beam output noise power

$$u = 1 + \frac{\gamma}{erP(1+\gamma)}$$

It is desired to compare the four adaptive beamformers (MVDR, subarrays, beam space, and EMVDR) to a conventional beamformer using the AGI metric. In order to illustrate the properties of the equations found in Table 4.1 three separate cases will be covered. The number of sensors is taken to be N = 32.

Table 4.1 Array gain improvement (AGI) for full array MVDR and beam space, subarray, and EMVDR reduced dimension beamformers.

Beamformer	Array Gain Improvement
Full Array MVDR	$1 + \frac{r^2L(1-L)}{1+rE}$
Beam Space MVDR	$1 + \frac{r^2L(E-L)}{1+rE}$
Subarray Beam Space MVDR	$e\left[1 + \frac{r^2LL_s(1-\bar{L}_s) + r(L-L_s\bar{L}_s)}{1+r\bar{L}_s}\right]$
Eigenvector Enhanced MVDR	$\frac{[(u-L)+(u-1)\gamma L(2+\gamma)]^2(1+rL)}{(1+rL)[u(1+\gamma L)+(u-1)\gamma L(1+\gamma)]^2-L(r+1)(1+\gamma)[(2u-1)(1+2\gamma L+\gamma^2 L)-\gamma(1+\gamma L)]}$

The first two cases as seen in Figures 4.1 and 4.2 have the interference in what would be the mainlobe of a conventional beam steered at the source. This is performed by setting the normalized

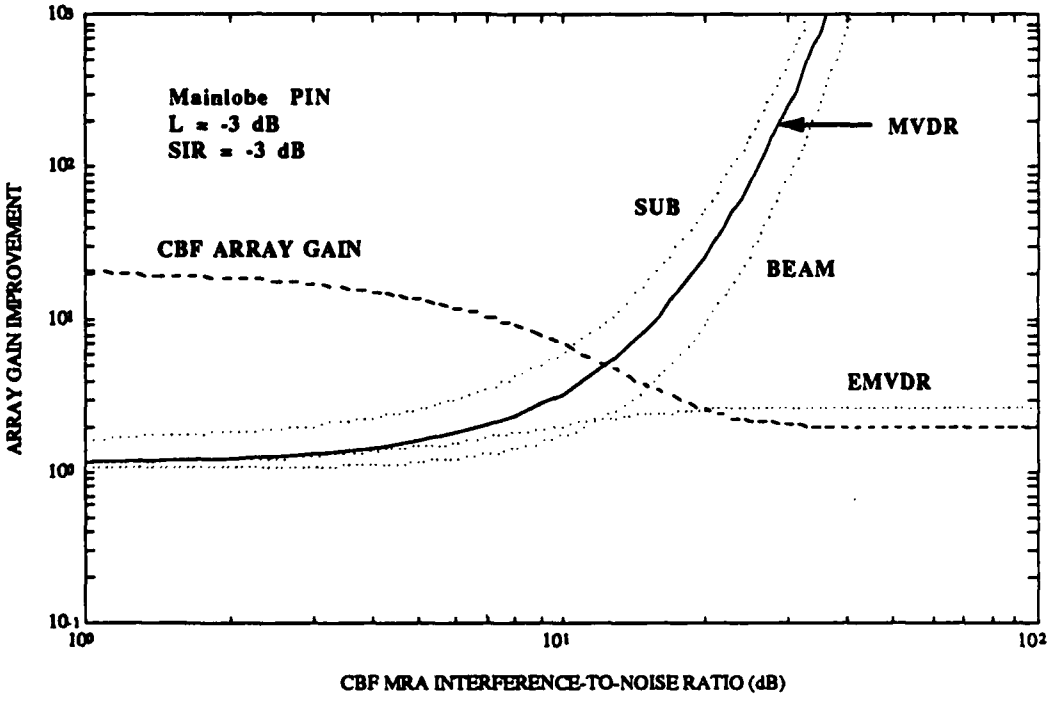

Figure 4.1 Array gain improvement (AGI) for a mainlobe point interference (PIN) with high signal-to-interference ratio.

interference level in the full array, L, to the level of the beampattern at the point where the PIN falls in the mainlobe. For Figures 4.1 and 4.2 the PIN falls at the -3dB point in the beampattern of a conventional beam steered at the source (L = -3dB). This means that if a conventional beamformer were steered to the direction that the source was arriving from, a signal coming from the direction of the interference would only be attenuated by 3dB. For strong interferences this is not very much attenuation.

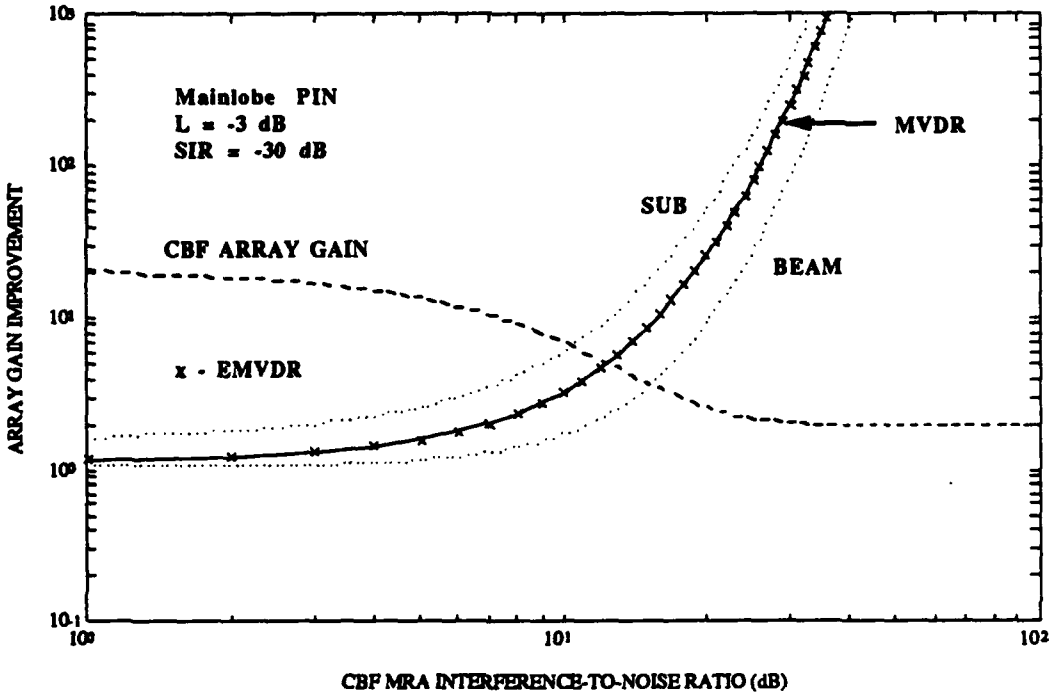

Figure 4.2 Array gain improvement (AGI) for a mainlobe point interference (PIN) with low signal-to-interference ratio.

In Figure 4.1 the signal to interference ratio is only P = -3dB. This means that the signal power is 3dB below the interference

power. Figure 4.2 shows the case where the signal power is 30 dB below the interference power (P = -30dB).

In Figure 4.3 the PIN is placed in the sidelobe of the conventional beamformer beampattern such that it receives 30dB of attenuation (L = -30dB). The signal to interference ratio is P = -10dB.

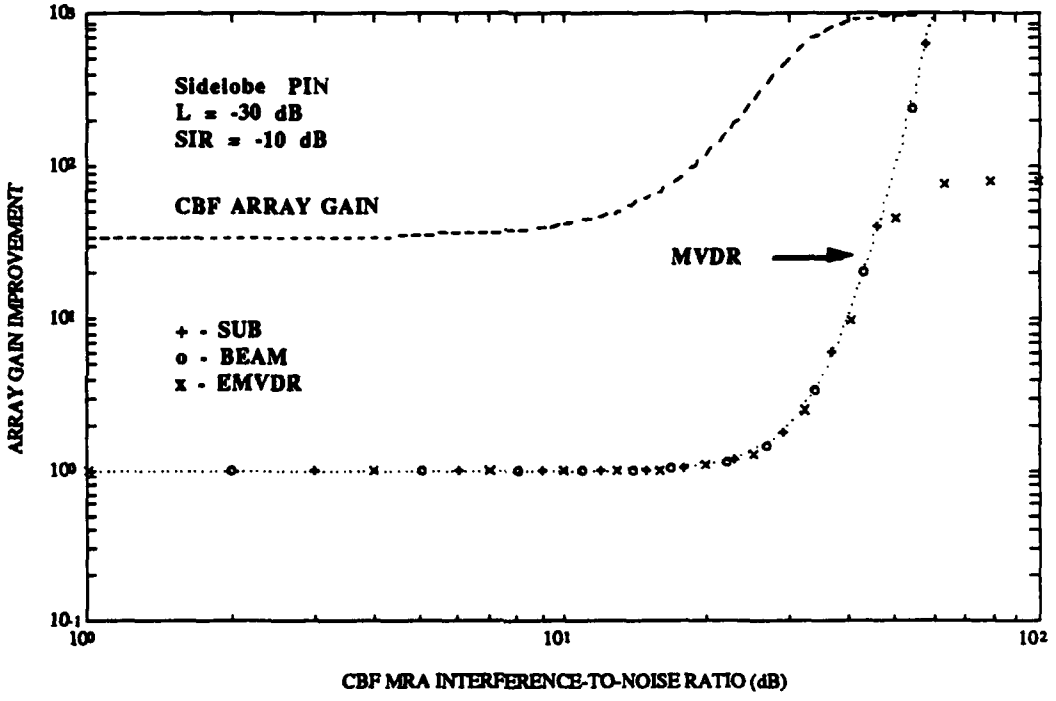

Figure 4.3 Array gain improvement (AGI) for a sidelobe point interference (PIN) with intermediate signal-to-interference ratio.

The AGI for the EMVDR beamformer was derived for the single source, single interference in uncorrelated background noise case. Only one dominant eigenvector and eigenvalue were used for the estimate of the CSDM. Figures 4.1 and 4.3 show the EMVDR beamformer reaching a plateau at high interference to beam output

noise power, r. The signal to interference ratio is -3 and -10 dB respectively in the figures. The signal is thus much higher than the background noise level for high r. Because of the strength of the signal it should also be assigned an eigenvector. This would improve the performance of the EMVDR beamformer to make it equivalent to that of the full array MVDR beamformer. When the signal power is much less than the interference power, as seen in Figure 4.2, or at low interference to beam output noise ratios the one eigenvector that is used to estimate the CSDM contains enough information to provide identical performance of the EMVDR and the full array MVDR beamformers.

Important conclusions to draw from these graphs are that the reduced adaptive dimension beamformers perform nearly as well, identically or better than the full array adaptive MVDR beamformer. This implies that the performance may be the same using a reduced adaptive dimension as when using the full MVDR beamformer. This statement must be clarified to include the condition that the reduced adaptive dimension provide enough degrees of freedom to deal with all the directional interferences present.

Figures 4.1 and 4.2 show how the adaptive beamformers provide substantial improvement over the CBF when the interference to noise ratio is high ($r > 10dB$). When the interfering signal is buried in the background noise ($r < 0dB$) the adaptive beamformers provide no improvement over a CBF, however there is also no degradation.

This implies that for low level or nonexistant interferences the adaptive beamformers perform the same as conventional ones.

4.2 Beampatterns

A common misconception about the beampatterns of high resolution beamformers concerns their mainlobe width. CBF beampatterns are often compared by their mainlobe width. An adaptive beamformer that provides greater resolution does not necessarily have a narrower mainlobe than its CBF counterpart. The effect of the adaptive beamforming is in the placement of the nulls that occur between each of the lobes in the beampattern. The MVDR beamformer places nulls such that the energy due to all the interferences is optimally cancelled. In order to illustrate this the example of Figure 4.1 is explored. The interference is at the -3dB point of a conventional beam, the signal to interference ratio is -3dB, and the interference to noise ratio is 15dB. The beamformers are pointed at the source which is placed at the broadside angle of zero degrees. The interference is at an angle of 1.58 degrees.

The even figures between 4.4 and 4.14 show the beampatterns for all arrival angles for six different beamformer configurations. The odd figures between 4.5 and 4.15 are an expanded plot of the area where the source and interference are located. The beamformer configurations are described in Table 4.2.

The beampatterns are formed assuming that perfect knowledge of the CSDM is available. This is the case of infinite time averaging or expected performance for a stationary scenario.

As seen in Figures 4.4 & 4.5 the conventional beamformer only attenuates the interfering signal by 3dB. All of the adaptive beamformers steer a null into the vicinity of the interference as shown by Figures 4.6 through 4.15. The gain the beampattern applies to the source angle of zero degrees is always unity. This is because of the distortionless response constraints imposed by all of the adaptive algorithms.

Table 4.2 Beamformer configurations for Figures 4.4-4.15.

Figures	Beamforming	Description
4.4 & 4.5	CBF	Uniform shading
4.6 & 4.7	Full array MVDR	
4.8 &4.9	Subarray	# Sensors per subarray = 8
		# Subarrays = 7
		Subarray shading = uniform
4.10 & 4.11	Beam space	# Interpolation beams = 5
4.12 & 4.13	EMVDR	Enhancement = 1
		# Eigenvectors = 1
4.14 & 4.15	EMVDR	Enhancement = 1
		# Eigenvectors = 2

The beampattern generated by the subarray preprocessing beamformer shows how the subarray beampattern is imposed on the true spectra of the energy impinging on the array. The resulting spectrum is then undersampled causing the aliasing as seen in Figure 4.8. The first groups of three lobes to either side of the main lobes

(-15 to -30 and 15 to 30 degrees) are the most adjacent repeated spectra that are aliased down into the original spectrum. Note that the beam space preprocessor produced a beampattern, Figures 4.10 & 4.11, almost identical to that of the full array MVDR beamformer.

The EMVDR beamformer in Figure 4.13 shows the null slightly closer to the source than the other adaptive beamformers. This is expected because the single eigenvector used in the enhanced estimate of the CSDM that forms the beamforming vector contains information about both the source and the interference. If the signal power were much smaller than the interference (it is only 3dB smaller in this example) it would be expected that the information about the source contained in the dominant eigenvector would be small compared to the information about the interference. Figures 4.14 and 4.15 show the beampattern generated by using two eigenvectors. Between the two eigenvectors all of the information about the interference is found and it is seen that the beampattern is identical to that of the full array MVDR beamformer.

4.3 Beam Responses

This section contains a comparison of the responses of each beamformer to a given scenario. Various scenarios are presented in order to illustrate some of the properties of the CBF, the full array MVDR beamformer, the subarray and beam space matrix preprocessor beamformers and the enhanced MVDR beamformer.

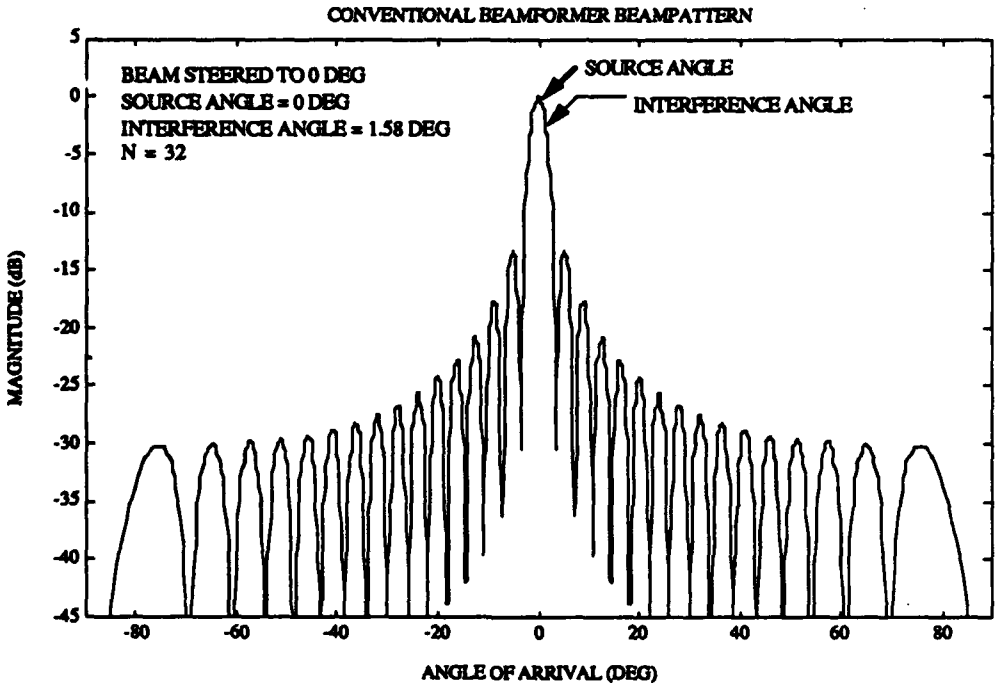

Figure 4.4 CBF beampattern, uniform shading, all arrival angles.

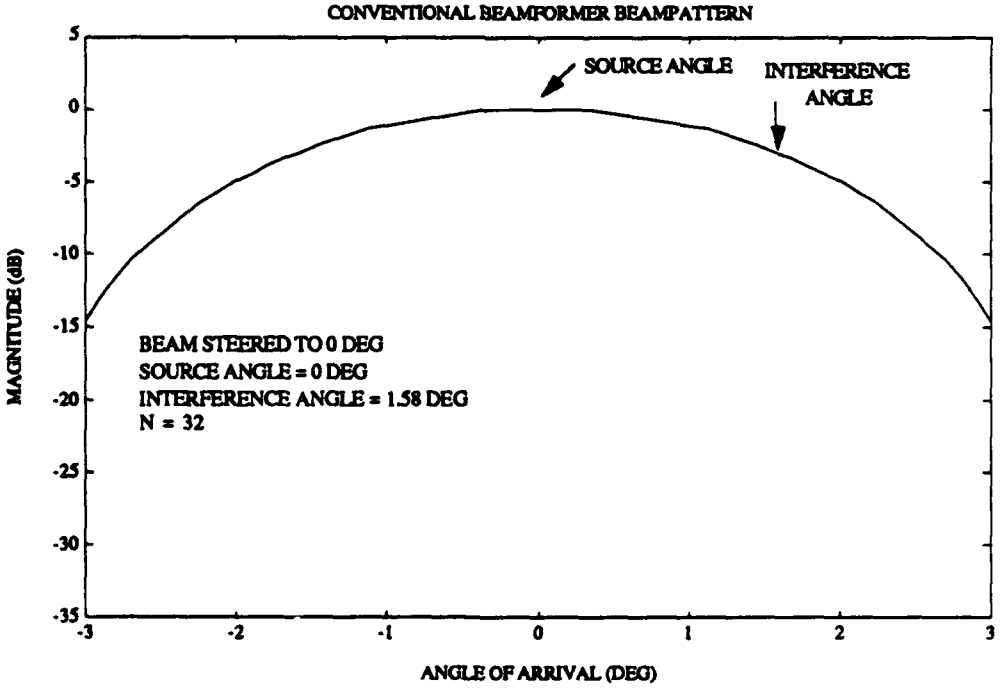

Figure 4.5 CBF beampattern, uniform shading, selected arrival angles.

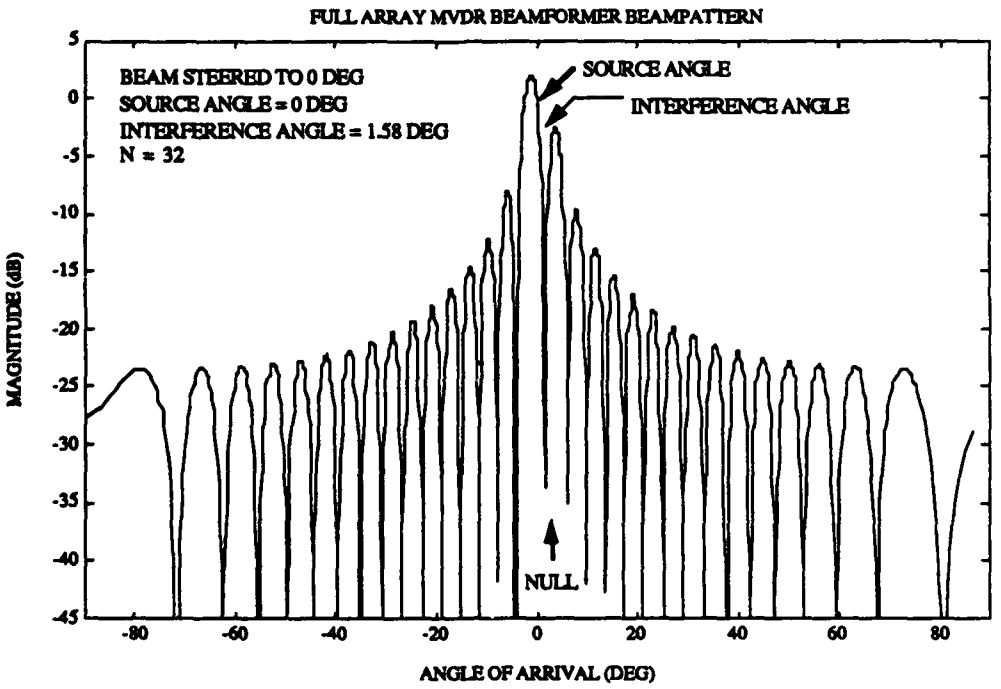

Figure 4.6 MVDR beampattern, all arrival angles.

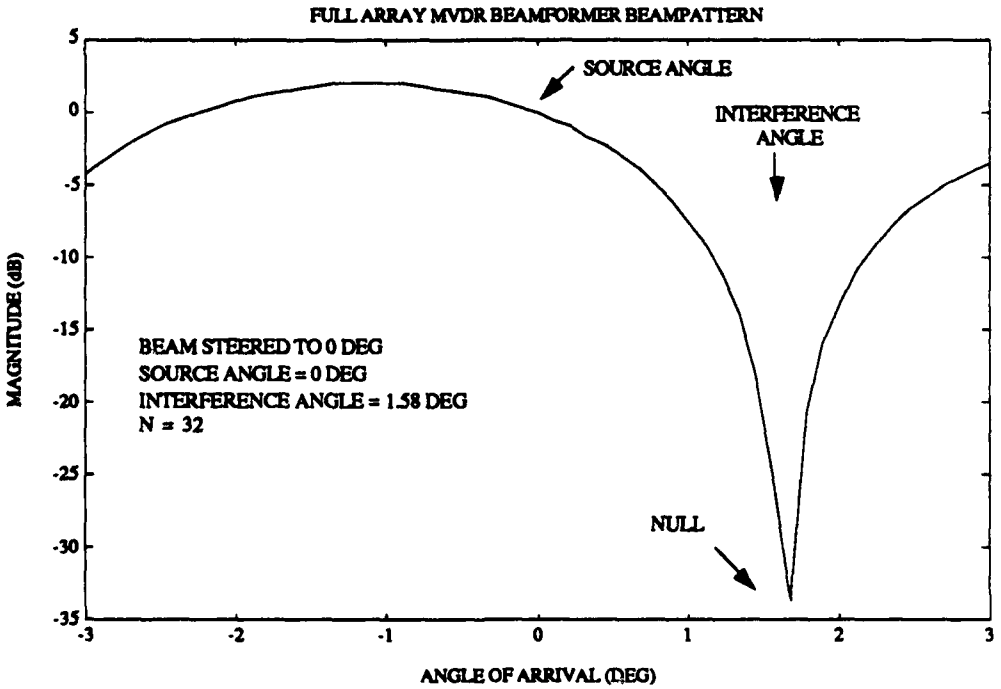

Figure 4.7 MVDR beampattern, selected arrival angles.

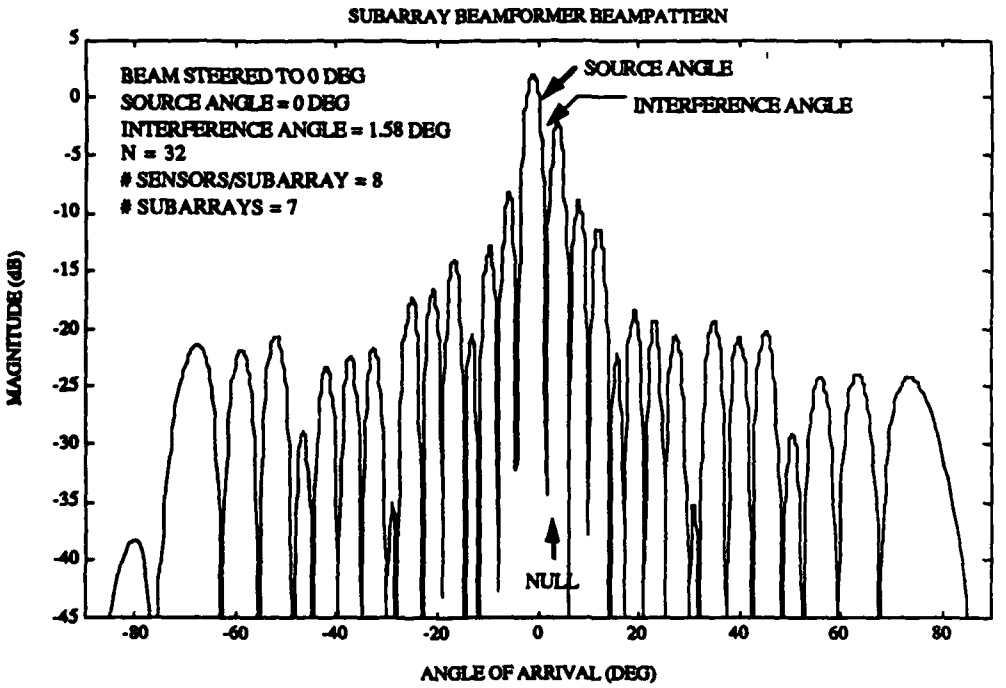

Figure 4.8 Subarray beampattern, all arrival angles.

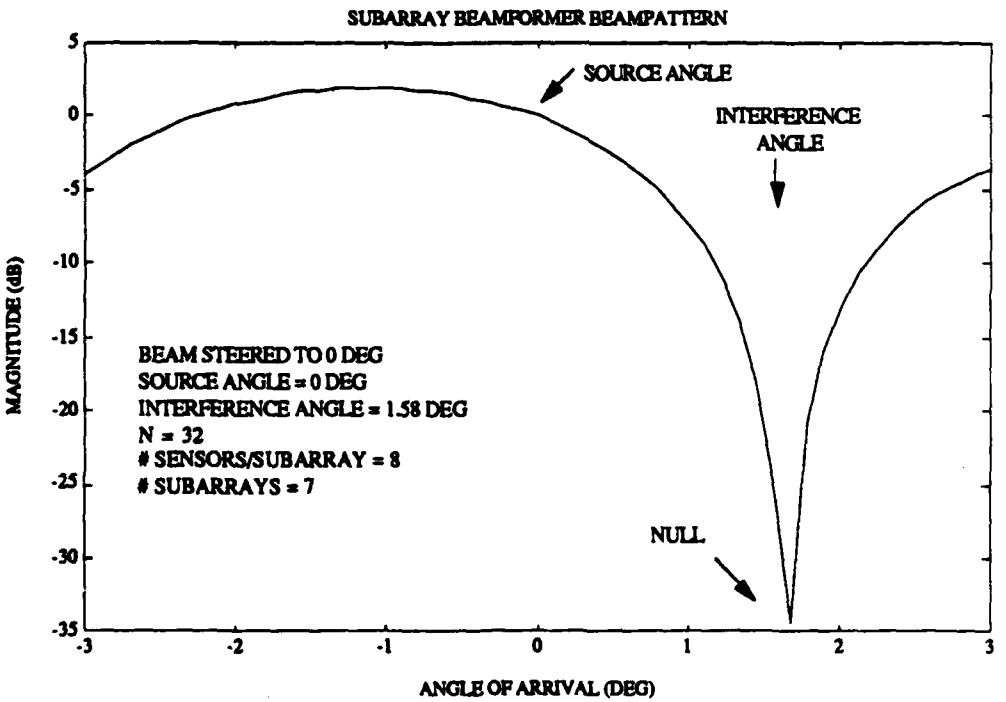

Figure 4.9 Subarray beampattern, selected arrival angles.

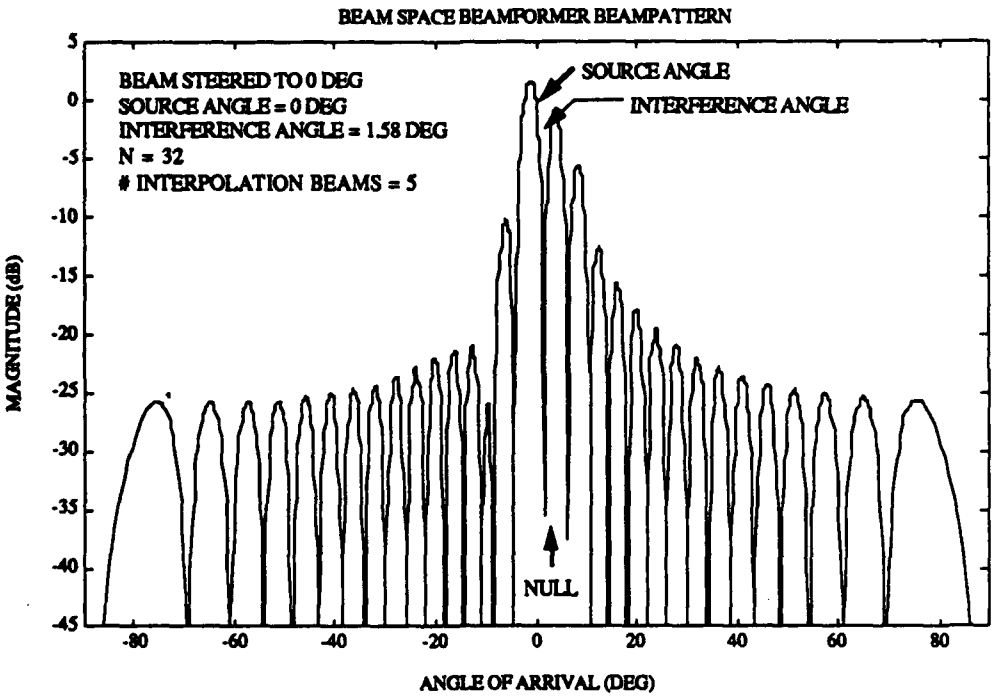

Figure 4.10 Beam space beampattern, all arrival angles.

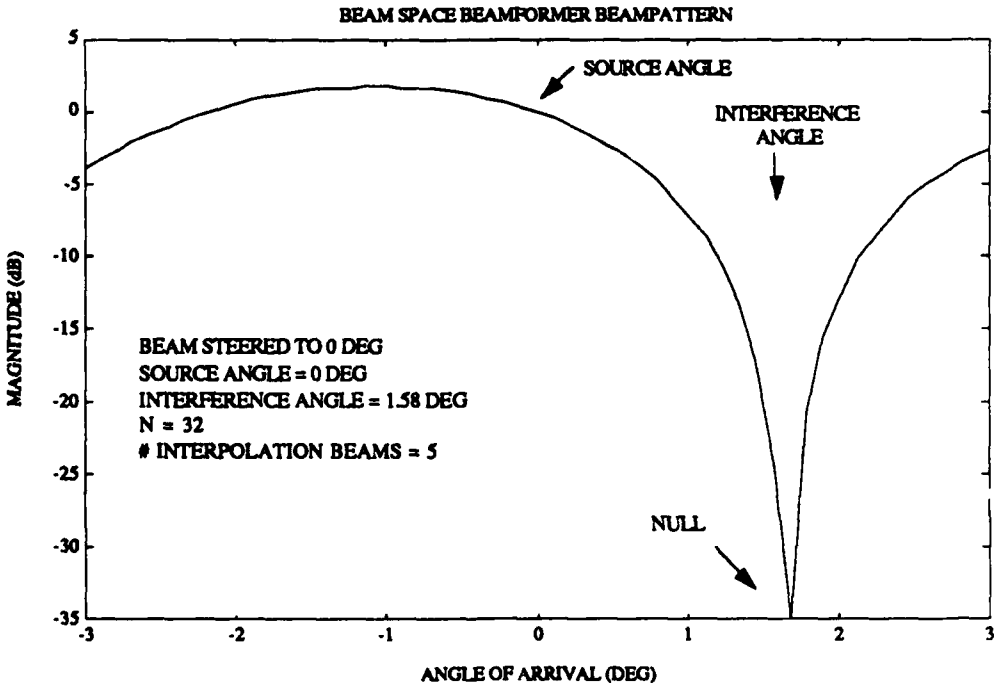

Figure 4.11 Beam space beampattern, selected arrival angles.

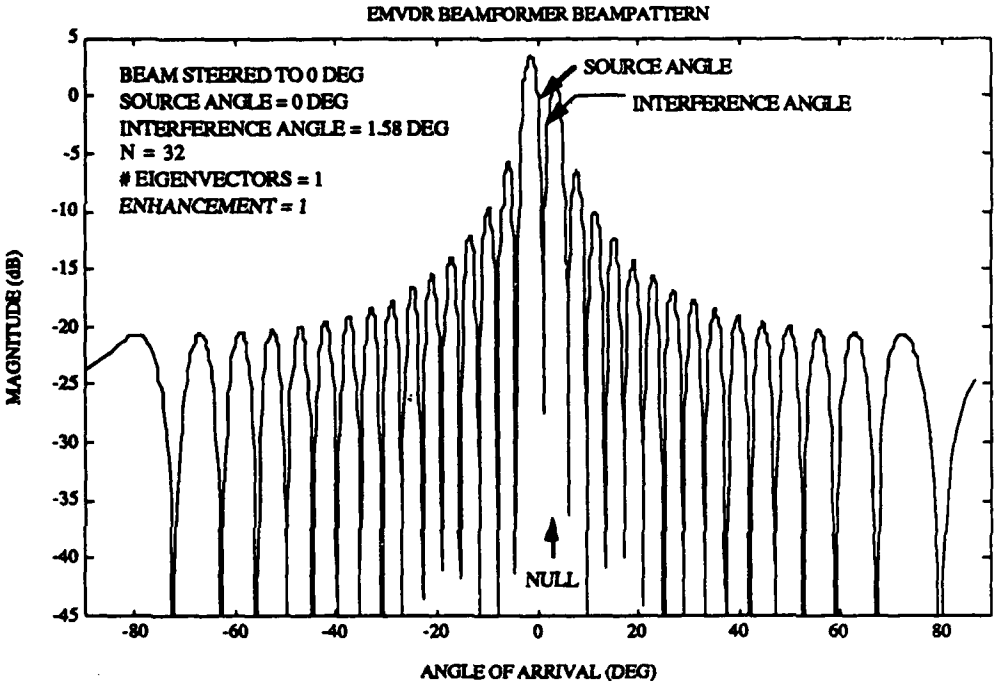

Figure 4.12 EMVDR beampattern, one eigenvector, all arrival angles.

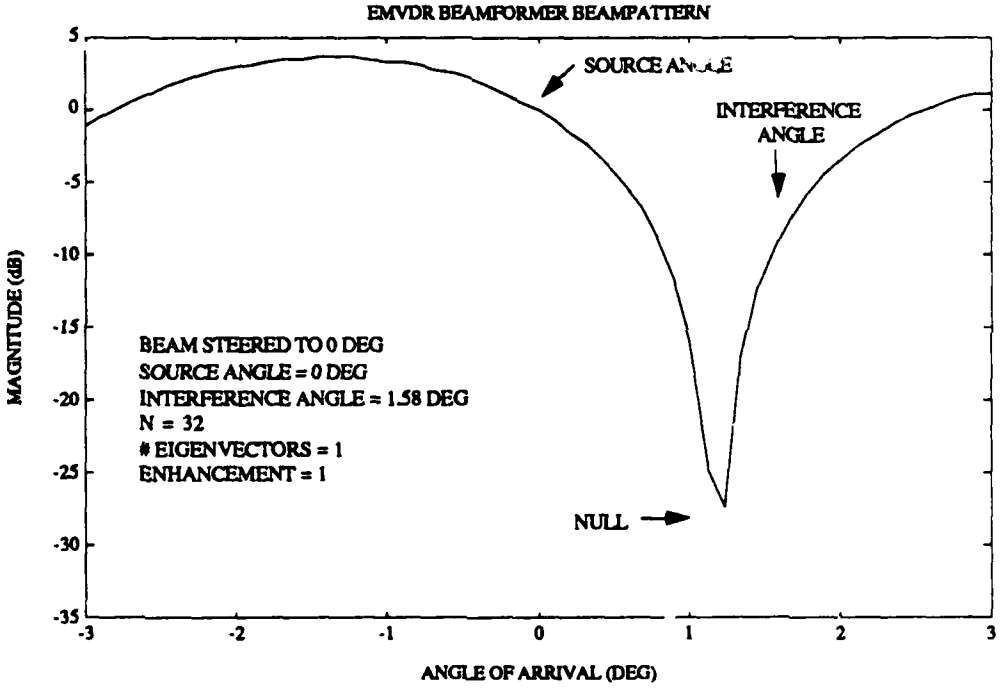

Figure 4.13 EMVDR beampattern, one eigenvector, selected arrival angles.

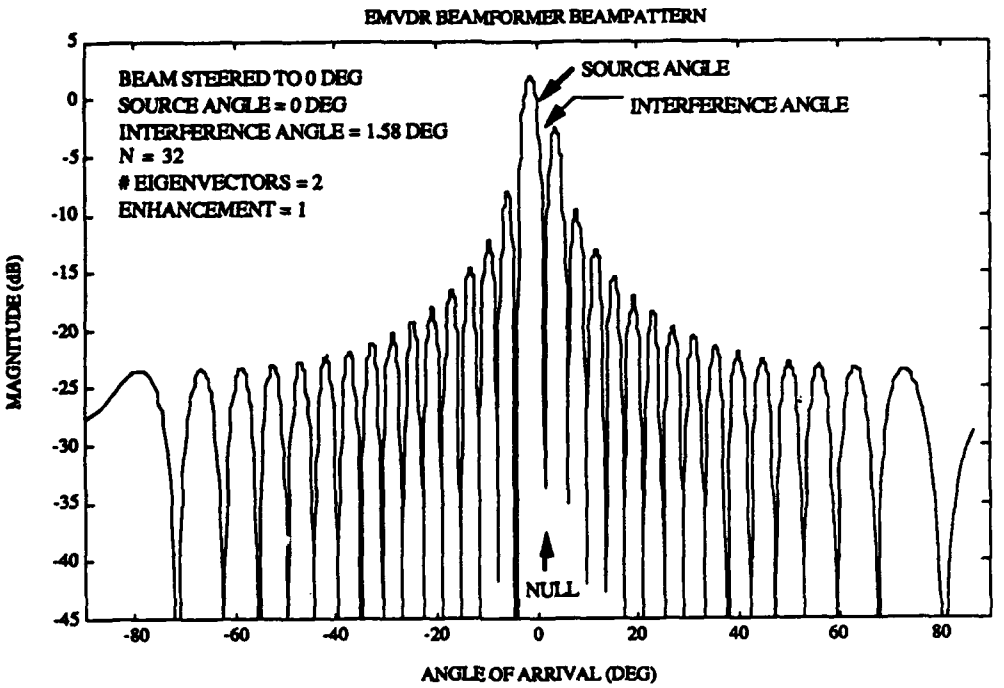

Figure 4.14 EMVDR beampattern, two eigenvectors, all arrival angles.

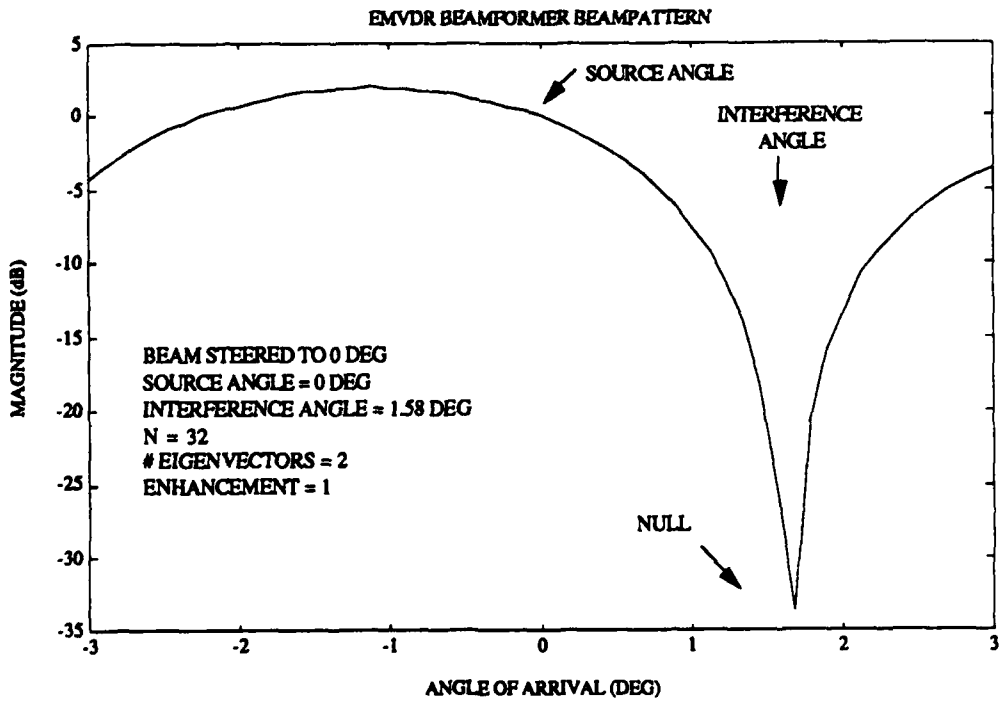

Figure 4.15 EMVDR beampattern, two eigenvectors, selected arrival angles.

The beamformers are driven by random data vectors that are generated according to the model discussed in Section 3.1. A plane wave source impinging on the line array has a complex random amplitude scaling the frequency steering vector pointing to the direction of the source. Uncorrelated complex background noise is added to the frequency data vector. Thus the beamformer input is a frequency data vector consisting of the sum of the steering vectors of each plane wave source scaled by a complex random number and a complex random noise vector. A sixteen sensor array with one-half wavelength spacing is beamformed at the design frequency of the array to look in 5*N = 80 beams equally spaced in wavenumber or sin(arrival angle) space.

The graphical output is in the form of an arrival angle versus time waterfall of beam responses. One trace in the time waterfall corresponds to the beam response of the beamformer steered to each of the 80 look directions for a particular time. The time increases upward in the waterfall where the first (bottom) trace corresponds to the beam response computed from the fifth update of the exponentially averaged CSDM or the eigen-structure. The last (top) trace is the beam response after fifty more updates to the CSDM or eigen-structure. This display structure is chosen to illustrate how the beamformers perform against random data. Underneath the waterfall plot each beam response plot is overlaid providing a form of an averaged beam response.

Each beam response trace is compressed to provide greater visual display capability. The compression formula is,

$$y = k\frac{\log_{10}(1 + mx/a)}{\log_{10}(1+m)}, \qquad 4\text{-}9$$

where y is the value plotted, x is the beam output power, m = 8, a = 1 and k = 10. The compression allows smaller signals to come through in a linear fashion (seen by approximating the compression function by a first order Taylor series). Larger signals are compressed by the log function. The end result is that low level signals may be seen in the presence of higher level ones.

The deflection or detection index, as described by Urick in [16], is computed for each plane wave source in the beam responses. Deflection is defined as,

$$d = \frac{(m_s - m_n)^2}{\sigma^2}, \qquad 4\text{-}10$$

where m_s and m_n are respectively the mean values of a signal and noise beam output where the averaging is over time and σ^2 is the variance of the noise beam output. The signal beam is the beam with an MRA nearest to the direction of arrival of the source of concern and the noise beam is placed such that little corruption occurs due to plane waves entering the sidelobes of the beampattern.

Table 4.3 Beam response case scenario descriptions.

Figure Number	Source One Strength (dB)	Source One Angle (degrees)	Source Two Strength (dB)	Source Two Angle (degrees)	Noise Power (dB)	Noise Beam (degrees)
4.16	0	0	-	-	-3.0	-85.0
4.17	0	0	-10.0	15.0	-3.0	-85.0
4.18	0	0	-10.0	45.0	-3.0	-85.0
4.19	0	0	-3.0	15.0	-3.0	-85.0
4.20	0	-45.0	0	0-50.0	-3.0	-85.0

Five different scenarios are used to compare the beamformers. The specifics about each case are described in Table 4.3.

Figures 4.16 through 4.20 show the graphical output of the beam responses. The CBF beam response is always shown as the baseline for performance as seen in the (a) position in each figure. The shading of the CBF beamformer is Chebyshev with 30 dB sidelobes. The full array MVDR beamformer is in the (b) position, the beam space beamformer with five interpolation beams is in the (c) position and the subarray beamformer with five subarrays of eight sensors each and 0.5 dB acceptable scalloping loss is in the (d) position. The subarray beams have Chebyshev shading with 30dB sidelobes. The (e) and (f) positions have the EMVDR beamformer beam responses. The (e) position is used when one dominant mode or eigenvector is used in the beamformer and the (f) position for the case of two dominant modes. The enhancement is always kept at unity to keep the deflection parameter equivalent to the other beamformers.

Table 4.4 contains the deflection parameters for the beam responses shown in Figures 4.16 through 4.20. The scenarios with two plane wave sources have deflections calculated for both sources. The source number shown in the first column of Table 4.4 corresponds to the source number shown in Table 4.3. The EMVDR beamformers are with one and two eigenvectors.

Table 4.4 Plane wave source deflections (dB) for beamformer outputs.

Figure/Source	CBF	MVDR	BEAM	SUB	EMVDR-1	EMVDR-2
4.16	29.20	30.69	25.79	30.54	32.17	-
4.17 / 1	27.82	29.80	27.21	28.95	30.39	31.31
4.17 / 2	14.87	11.50	8.14	11.00	10.64	11.67
4.18 / 1	27.61	29.52	26.41	28.83	30.26	30.16
4.18 / 2	9.39	11.81	7.46	10.85	11.07	11.97
4.19 / 1	28.29	30.05	27.17	28.90	32.00	32.20
4.19 / 2	25.39	25.24	22.14	24.48	24.93	26.49
4.20	18.97	27.93	25.48	27.00	28.64	25.42

Fifty time samples are used to estimate the means and variances of the noise and signal beams. The time samples used are the ones shown in the figures. The first time sample shown is generated from the fifth update of the CSDM or eigenvector estimator. This is to remove the deflection computation from most of the effects of the initialization of the CSDM and eigenvectors.

Several important points may be drawn from the examples shown in Figures 4.16 through 4.20 and are encapsulated in the following summary:

- Almost all of the adaptive beamformers resolved the plane wave sources to a finer bearing than the conventional beamformer. The exception is when an eigenvector was not attributed to a plane wave source and conventional beamforming was performed in the EMVDR beamformers. In this case the resolution is equivalent to that of a uniformly shaded conventional beamformer.

- A low level source is more clearly seen in the presence of a high level interference for all of the adaptive beamformers (see Figure 4.17). The deflection of the low level source in Figure 4.17 is greatest for the case with two eigenvectors. This is expected because of the high resolution obtained by the EMVDR beamformer for signals that have eigenvectors assigned to them. The next largest deflection is the CBF. This is not expected and the larger deflection is attributed to energy entering the mainlobe or sidelobes of the conventional beamformer, steered at the low level source, from the interference at zero degrees. This will cause the mean of the signal beam output to increase and correspondingly an increase in the deflection.

- A very important aspect of the EMVDR beamformer is apparent in Figures 4.19(e) and 4.20(e) where the high level signals that have eigenvector assignment are very finely resolved. All other angles have conventional beamforming characteristics with the added removal of the interfering signal.

- Figure 4.20 shows a scenario with a moving source. The source changes bearing from zero degrees to fifty degrees in fifty time samples, a rate of one degree per time sample. The CBF, MVDR, subarray and beam space beamformers track the source movement well as seen in Figure 4.20(a)-(d). The EMVDR beamformer, in Figure 4.20(e), with one eigenvector (assigned to the stationary source) allows conventional beamforming of the moving source and adequate tracking. When an eigenvector is assigned to the moving source, as seen in Figure 4.20(f), the eigenvector estimation algorithm would not track the changing eigenvector. This may be due to an incorrect averaging constant that controls the amount of new data that is used by the eigenvector estimator. A detailed analysis of the eigenvector estimation algorithm is required before any firm conclusions may be drawn. Note that this questionable result does not detract from the EMVDR beamforming algorithm for other methods of obtaining the eigen-structure of the CSDM are available.

- In [4] the beam space and subarray matrix preprocessors showed a scalloping that occurred on the infinite time averaged, or perfectly known CSDM, beam response. The scalloping is due to the subarray conventional beam formation and the attenuation incurred on any signals not arriving on the MRA of the subarray beam. In the beam space algorithm the full array conventional beams in the preprocessing are what causes the scalloping. Note that the scalloping is not apparent in the beam responses to random data.

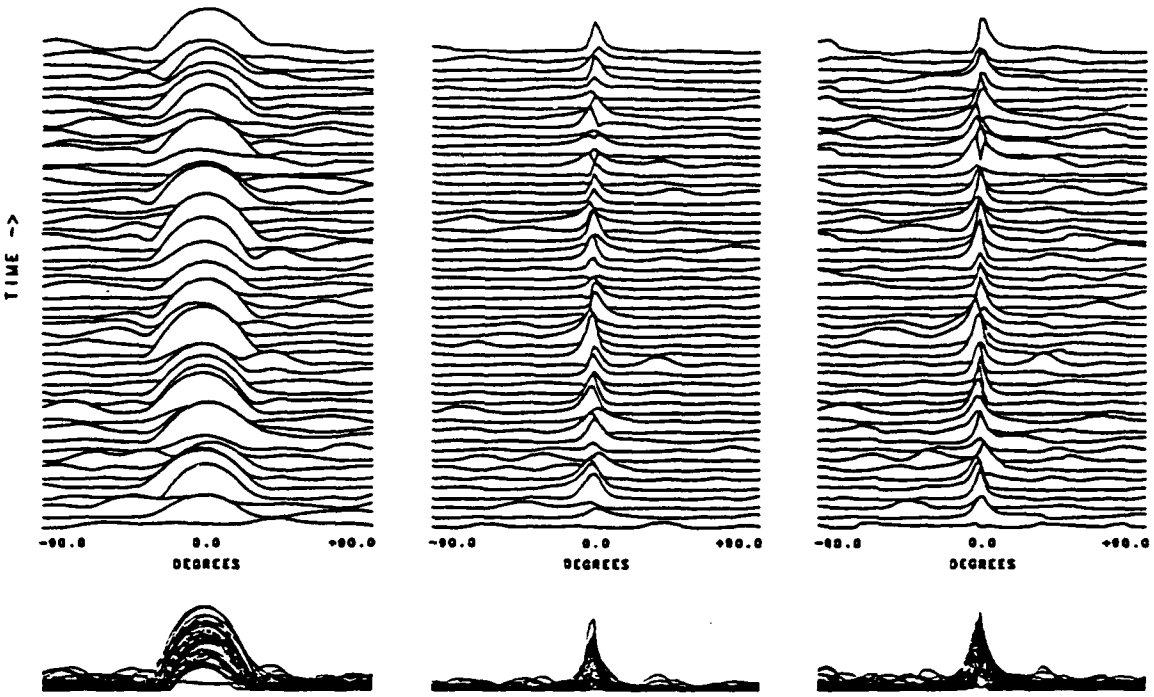

(a) CBF (b) Full array MVDR (c) Beam space

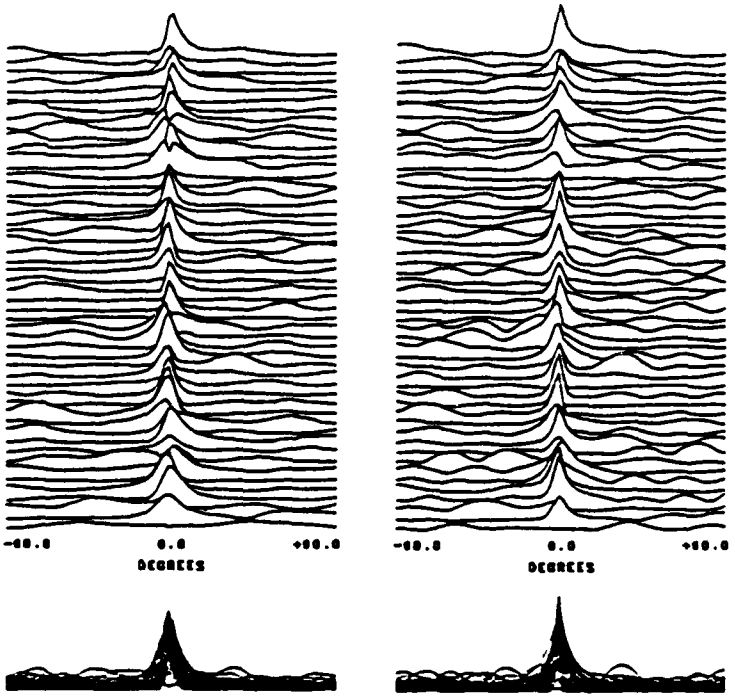

(d) Subarray (e) EMVDR, D=1

Figure 4.16 Beam response - Single source

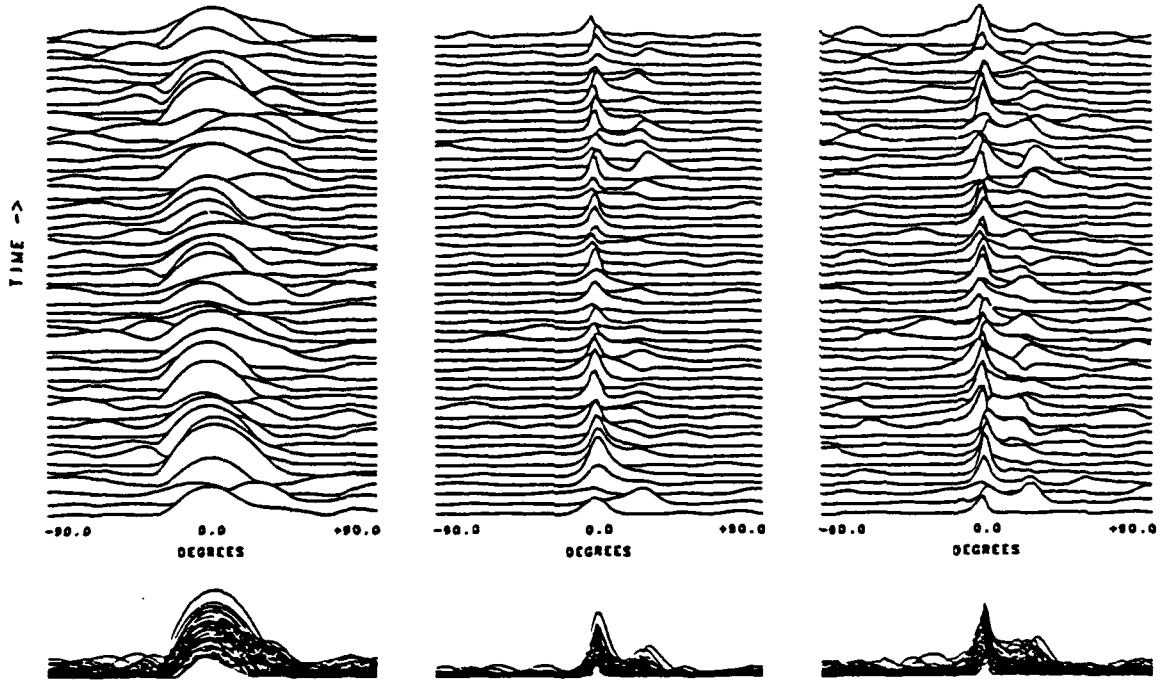

(a) CBF (b) Full array MVDR (c) Beam space

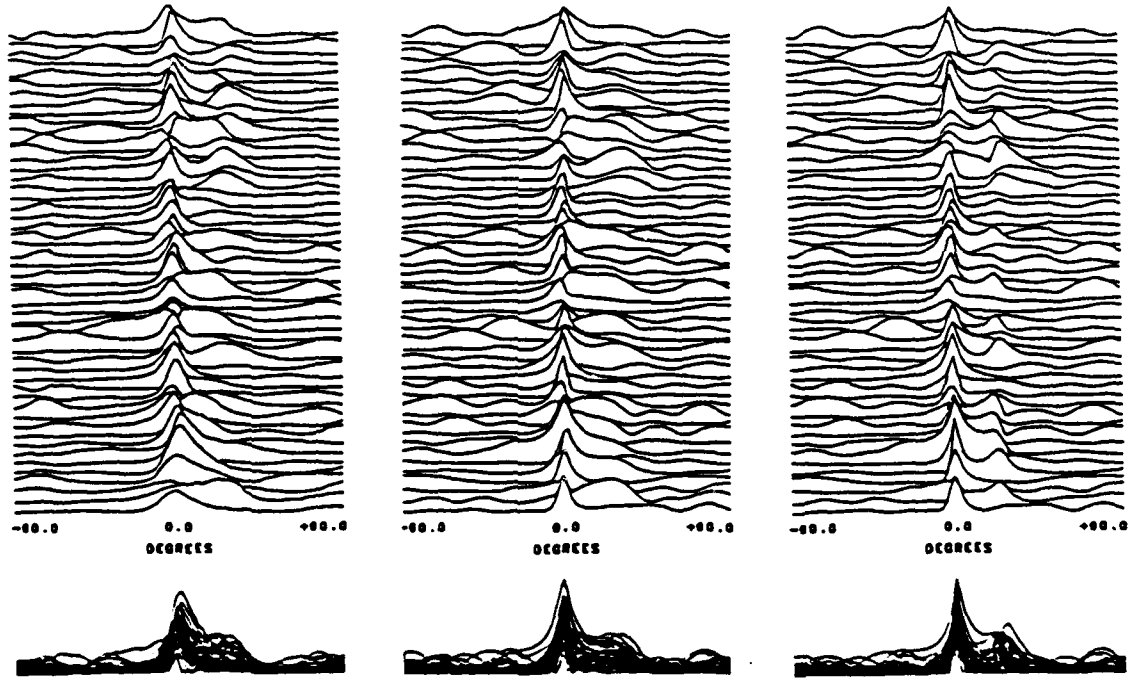

(d) Subarray (e) EMVDR, D=1 (f) EMVDR, D=2

Figure 4.17 Beam response - Single source, mainlobe interference, SIR = -10dB

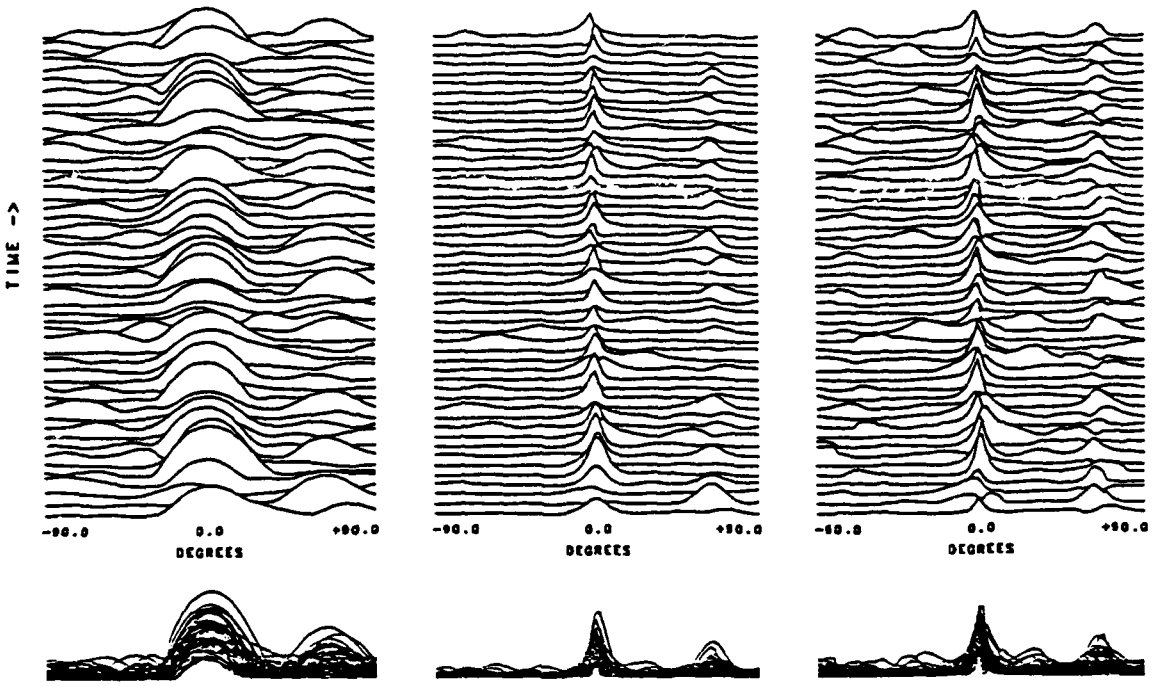

(a) CBF (b) Full array MVDR (c) Beam space

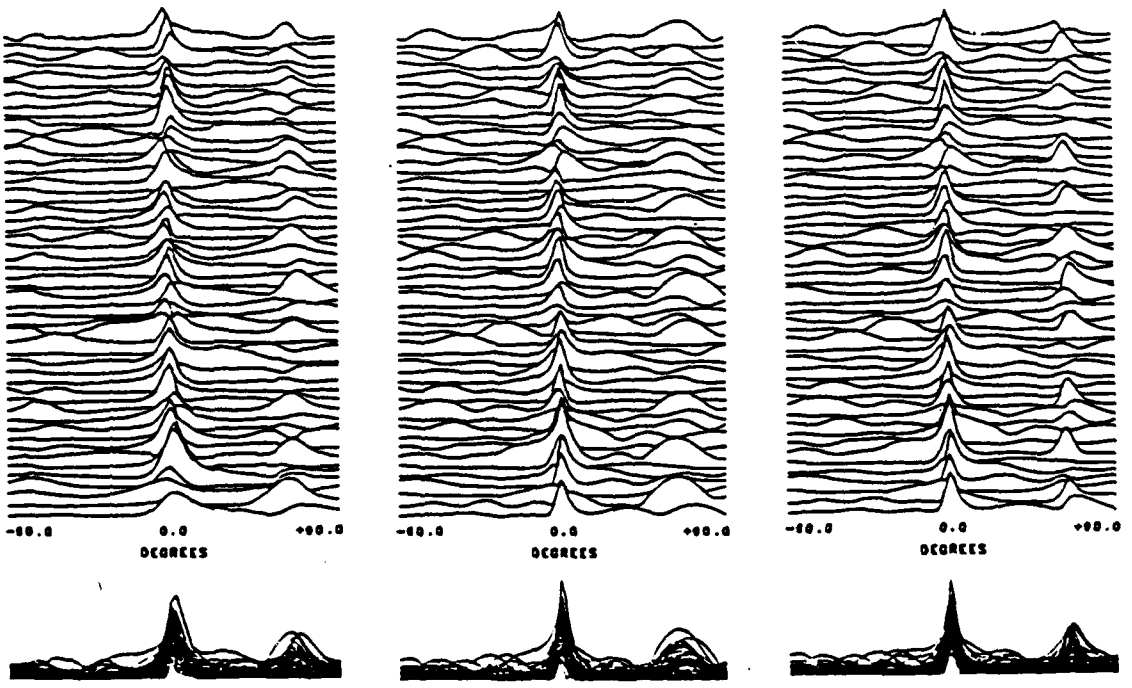

(d) Subarray (e) EMVDR, D=1 (f) EMVDR, D=2

Figure 4.18 Beam response - Single source, sidelobe interference, SIR = -10dB

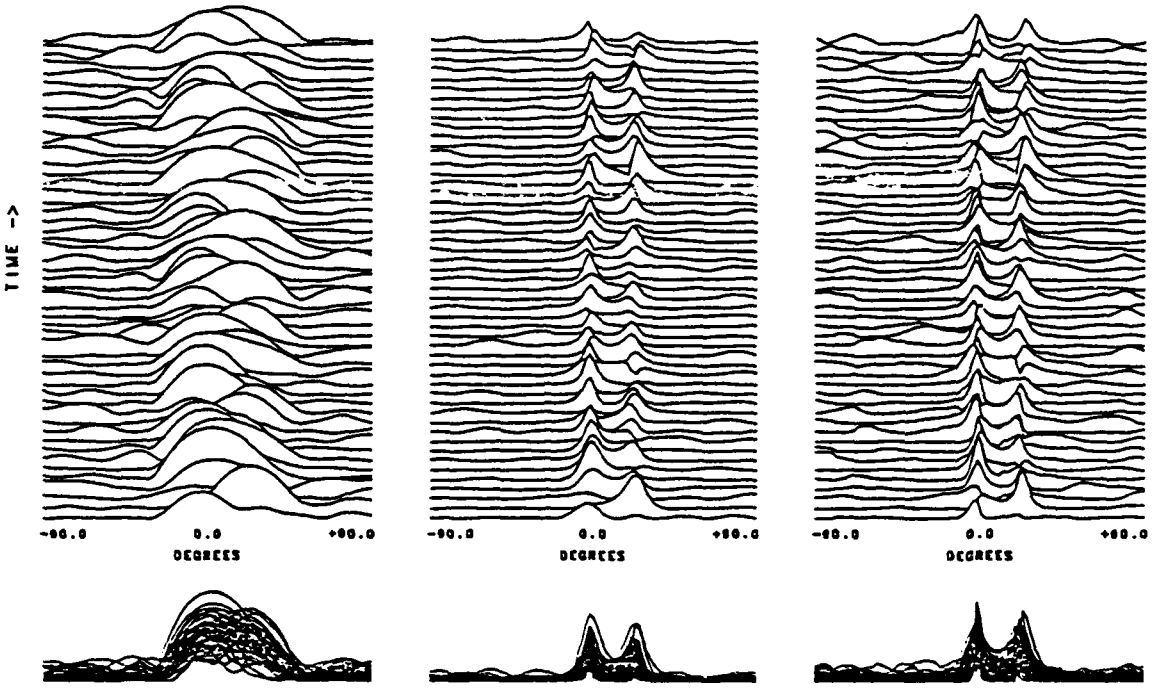

(a) CBF (b) Full array MVDR (c) Beam space

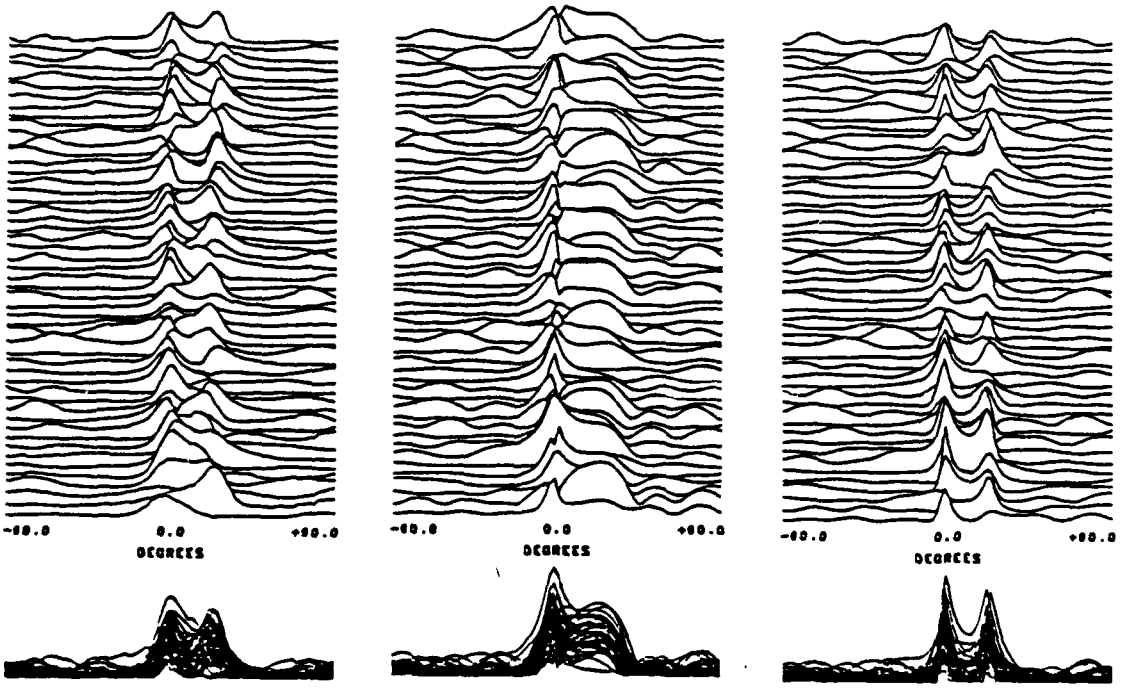

(d) Subarray (e) EMVDR, D=1 (f) EMVDR, D=2

Figure 4.19 Beam response - Single source, mainlobe interference, SIR = -3dB

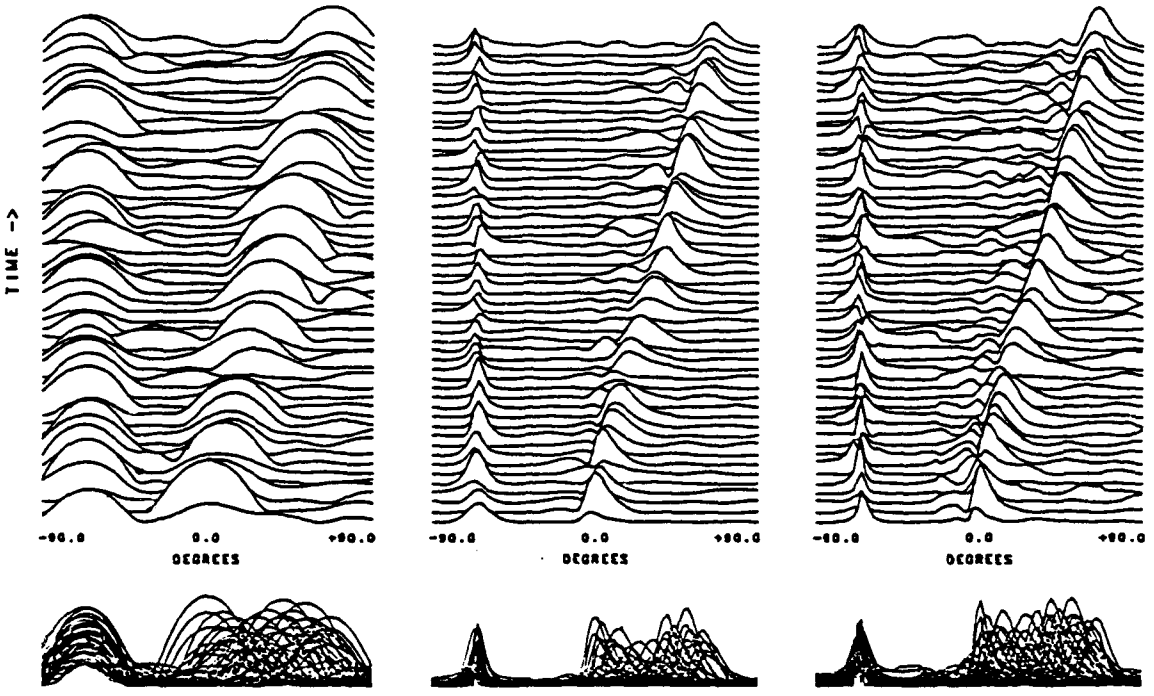

(a) CBF (b) Full array MVDR (c) Beam space

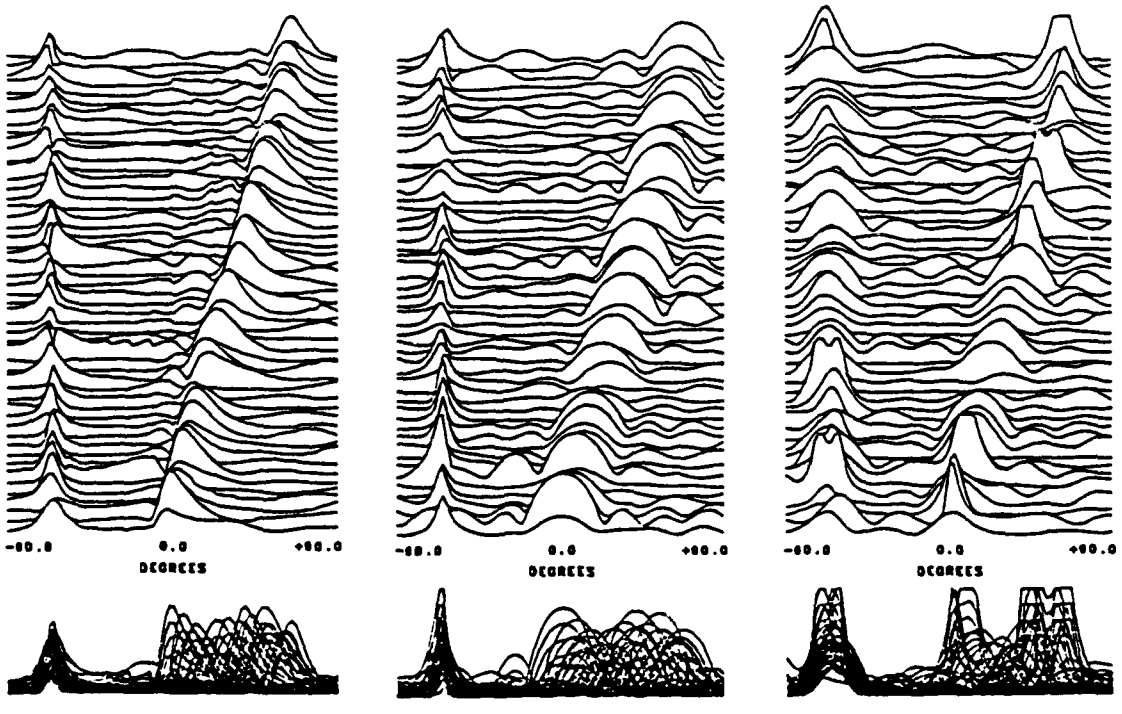

(d) Subarray (e) EMVDR, D=1 (f) EMVDR, D=2

Figure 4.20 Beam response - One stationary source, one moving source

4.4 Numerical Intensity

The full array MVDR beamformer requires on the order of N^2 numerical operations per update per beam as shown by Owsley in [2] and [4]. The inversion of the estimated CSDM is the driving factor behind the numerical intensity. The reduced adaptive dimension beamformers all alleviate this problem to varying extents. As seen in [4] and Table 4.5 the numerical complexity is a function of the following parameters:

MVDR, CBF, and all others:

- N - Number of sensors in the array
- L_b - The total number of beams to form, nominally = 5N

Beam space:

- M - The number of interpolation beams

Subarrays:

- M - The number of subarrays
- N_s - The number of sensors per subarray
- L_s - The number of subarray beams to form

EMVDR:

- D - The number of dominant modes or eigenvectors used

Table 4.5 Beamformer complexity expressed in the number of arithmetic operations per update.

Beamformer	Numerical Complexity
CBF	NL_b
MVDR	$N^2 + N^2L_b + NL_b$
Beam space	$N^2 + 2M^2N + M^2L_b + ML_b$
Subarray	$N_sML_s + 2M^2L_s + M^2L_b + ML_b$
EMVDR	$DN + DNL_b + NL_b$

The numerical gain achieved by the use of a beamformer other than the full array MVDR beamformer may be calculated by taking the ratio of the number of operations per update for the full array MVDR beamformer to the required number of operations per update for the topic beamformer. For each of the beamformers of the beam response comparison of Section 4.3 the numerical gain is computed using the equations found in Table 4.5 and displayed in Table 4.6.

From this comparison it is seen that the EMVDR beamformer with one eigenvector achieves the most numerical gain. The beam space and then the subarray beamformers follow slightly behind it. The adaptive dimension of the subarray beamformer, the number of subarrays, was taken to be equal to that of the beam space algorithm, the number of interpolation beams. Fewer subarrays or fewer interpolation beams will provide greater numerical gain and varying performance. The price of optimal and sub-optimal beamforming is seen by the large numerical savings achieved by using conventional beamforming.

Table 4.6 Numerical gain for beamformers of Section 4.3.

Beamformer	Gain
CBF	17.2
MVDR	1.0
Beam space	6.4
Subarray	5.7
EMVDR, D=1	8.5
EMVDR, D=2	5.7

CHAPTER 5 - CONCLUSION

5.1 Summary

This thesis provides a general introduction to the concept of conventional and adaptive beamforming in Chapter 2 with a proposal for reducing the dimension of the adaptive process in adaptive beamforming.

The theoretical development of the matrix preprocessed minimum variance distortionless response (MVDR) beamformer is presented in Chapter 3 as well as the beam space and subarray matrix preprocessing schemes. The enhanced minimum variance beamformer is developed in Section 3.4.

A comparison of the three topic reduced dimension adaptive beamformers with the full element space MVDR algorithm and a conventional beamformer is shown in Chapter 4. The comparison is accomplished using such metrics as the array gain improvement (AGI), the beamformer beampatterns, beam responses and numerical complexities.

The AGI and beampattern comparisons have both shown for the single source, single interference in uncorrelated background noise scenario that the reduced adaptive dimension beamformers provide nearly the same average performance as the full array MVDR beamformer. The beam response comparisons have confirmed

this in terms of the deflection parameter and by visual inspection of the graphical output of the beamformers shown in Section 4.3.

The enhanced minimum variance beamformer (EMVDR) showed equivalent performance (when the correct number of eigenvectors is used) in the AGI and beampattern comparisons. In the beam response comparisons the EMVDR beamformer consistantly outperformed the MVDR beamformer in terms of deflection and visual inspection of the graphical output. There are still two areas of concern associated with the EMVDR beamformer: the required estimation of the number of plane wave interferences and further exploration of the eigen-structure estimator used and other potential estimators.

The subarray and beam space reduced adaptive dimension beamformers performed nearly as well as but not better than the MVDR beamformer in terms of deflection and visual inspection of the graphical output. The beam space beamformer has an advantage over the other adaptive beamformers in that access to the sensor level data is not required. The subarray beamformer may prove more tolerant to array sensor position perturbations than the other adaptive beamformers.

5.2 Future Work

Several areas of interesting work deserving greater depth have been highlighted throughout this thesis. The following paragraphs are devoted to listing these areas.

The EMVDR beamformer proved to be the most interesting and also the most unfinished of the beamformers evaluated. One primary concern of the beamformer is the number of dominant modes required to achieve the best performance. The AGI comparison in Section 4.1 shows that only the strong plane wave sources need to be attributed eigenvectors. If fewer eigenvectors are used the performance degrades some but as seen in the beam response comparisons of Section 4.3, particularly Figure 4.19(e), it may be possible to start out with fewer eigenvectors than required and increase the number after visual evaluation of the beam response. The noted figure clearly shows a strong plane wave source being beamformed conventionally in the beam response plot. Once this is attributed an eigenvector, as in Figure 4.19(f), the beam response does not exhibit any obviously strong plane wave sources with conventional beamforming. It may be possible to automate this process removing the human interface. The estimate of the number of dominant plane wave sources must be constantly updated for the scenario may be changing.

The second concern of the EMVDR beamformer is the method of estimating the eigen-structure of the CSDM. Ideally the eigenvectors

and eigenvalues of an exponentially averaged CSDM are desired. This will allow equivalent comparison of the EMVDR beamformer with other beamformers utilizing the exponential CSDM averager. The one used in the simulations of this thesis, as described by Yang and Kaveh in [7] and in Appendix B, is numerically very quick and may provide the desired quality but requires further exploration.

As mentioned in the conclusions section, the subarray beamformer may be more tolerant to array sensor position perturbations than the other beamformers. When the exact position of the sensors in the array is not known and the position may be estimated for sections of the array the subarray technique may be ideally suited to the beamforming task for the perturbed array. The subarray size may be matched to the section whose location is known and then beamformed conventionally. Those beam outputs are then combined adaptively with the extra information about the section postitions.

A further application of the subarray preprocessing may be the use of the EMVDR beamformer at the subarray beam output stage instead of the MVDR process. This would further reduce the numerical intensity but would require a good algorithm for estimating the number of dominant plane waves in each subarray beam output.

The CSDM being estimated in the matrix preprocessed reduced dimension adaptive beamformers is of a smaller dimension than that of the full array MVDR beamformer. This may provide a reduced noise variance on a beam output due to the uncertainty of the CSDM estimation. This has not been shown in this thesis and is still a conjecture, however it is expected that the estimation of the smaller dimension CSDM should require a shorter time constant in the exponential estimator than the estimation of the full CSDM. Faster adaptation or lower variance beam outputs may be achievable because of the shorter time constant. Further work in this area should explore the estimation of the reduced dimension covariance.

As a group beamformers are subjected to queries about their performance against several debilitating scenarios such as angularly extended noise, correlated plane wave sources and scenarios that change over time. The reduced dimension beamformers may contain a facet that aids in the battle against these types of problems. Only further study will provide answers to these queries.

APPENDIX A - Cross Spectral Density Matrix Update and Inversion

UPDATE EQUATION

The covariance or cross spectral density (CSDM) matrix is not known a priori and must be estimated. It is defined as the expected value of the outer product of the frequency data vector with its complex conjugate transpose (tranjugate). In order to reduce noise associated with the estimation of the CSDM some sort of averaging is required. Block averaging estimates the CSDM as the sample mean of the outer products of L frequency data vectors,

$$\hat{\mathbf{R}} = \frac{1}{L} \sum_{i=1}^{L} \mathbf{x}(i,f)\mathbf{x}^{H}(i,f) \ . \qquad \text{A1}$$

This method requires L frequency data vectors to generate one CSDM estimate.

An alternative method is to perform exponential averaging of the stochastic rank one approximation to the CSDM yielding,

$$\hat{\mathbf{R}}(k) = (1-\alpha)\mathbf{x}(k,f)\mathbf{x}^{H}(k,f) + \alpha\hat{\mathbf{R}}(k-1) \ , \qquad \text{A2}$$

where α is the exponential averaging constant and varies between zero and one. This algorithm requires an initialization value for the CSDM. A block average, as shown above, the identity matrix, or an intelligent estimate based on the dominant plane wave sources and the structure of the CSDM may be used.

The minimum variance distortionless response (MVDR) beamforming algorithm requires the inverse of the CSDM multiplied by a known vector. A matrix inversion requires on the order of N^3 numerical operations. For large values of N this is not acceptable. Owsley covers in [2] and [5] the use of the Cholesky square root factorization of the CSDM in the update equation, A2, above. In [2] Owsley shows that the triangular Cholesky square root factorization yields an order of N^2 numerical operation algorithm for determining the MVDR beamforming vector. The Cholesky square root factorization of the CSDM is defined as,

$$\hat{\mathbf{R}}(k) = \mathbf{C}(k)\mathbf{C}^{H}(k), \qquad A3$$

where $\mathbf{C}(k)$ is the Cholesky square root factor of the estimated CSDM at time k. Brogan shows in [6] that the Cholesky square root factorization of a symmetric positive definite matrix exists and is a lower triangular matrix. Applying the Cholesky square root definition of the CSDM to the equation A2 above yields,

$$\hat{\mathbf{R}}(k) = (1-\alpha)\mathbf{x}(k,f)\mathbf{x}^{H}(k,f) + \alpha\mathbf{C}(k-1)\mathbf{C}^{H}(k-1). \qquad A4$$

Now by rewriting the above equation as the product of an N-by-N+1 matrix and its tranjugate,

$$\hat{\mathbf{R}}(k) = \left[\ \sqrt{1-\alpha}\ \mathbf{x}(k,f)\ \ \sqrt{\alpha}\mathbf{C}(k-1)\ \right]\left[\ \sqrt{1-\alpha}\ \mathbf{x}(k,f)\ \ \sqrt{\alpha}\mathbf{C}(k-1)\ \right]^{H}$$

$$= \mathbf{U}(k)\mathbf{U}^{H}(k). \qquad A5$$

Note that the N+1-by-N matrix $\mathbf{U}^{H}(k)$ is in the form of a row vector appended to the top of an upper triangular matrix.

$$\mathbf{U}^{H}(k) = \begin{bmatrix} \sqrt{1-\alpha}\,\mathbf{x}^{H}(k,f) \\ \\ \sqrt{\alpha}\mathbf{C}^{H}(k-1) \end{bmatrix} \qquad A6$$

If the diagonal of the upper triangular matrix were "zeroed out" then the bottom row would be a zero row vector and may be dropped yielding an N-by-N upper triangular matrix.

The diagonal of the matrix $\mathbf{C}^{H}(k-1)$ in A6 may be "zeroed out" by the use of a set of Givens rotations (see Golub & Van Loan [13]). The Givens rotation is an orthogonal matrix premultiplier that has the ability to zero out an array element. The Givens premultiplication matrix is in the form of an N+1-by-N+1 identity matrix with a two-by-two matrix slid along the diagonal. The two-by-two matrix is chosen to annihilate the diagonal elements of the $\mathbf{C}^{H}(k-1)$ matrix. The orthogonality of the Givens rotation matrix allows the preservation of the $\mathbf{U}(k)\mathbf{U}^{H}(k)$ product in equation A5. The N Givens rotations produce the following,

$$\hat{\mathbf{R}}(k) = \mathbf{U}(k)\mathbf{P}_1\mathbf{P}_2\cdots\mathbf{P}_N\mathbf{P}_N^H\cdots\mathbf{P}_2^H\mathbf{P}_1^H\mathbf{U}^H(k) \qquad \text{A7}$$
$$= \mathbf{U}(k)\mathbf{P}\mathbf{P}^H\mathbf{U}^H(k),$$

where,

$$\mathbf{P} = \mathbf{P}_1\mathbf{P}_2\cdots\mathbf{P}_N$$
$$\mathbf{P}_i\mathbf{P}_i^H = \mathbf{I}_{N+1}\ .$$

It is desired to form the update equation of the CSDM into a Cholesky square root factorization form. Once all the diagonal elements of $\mathbf{C}^H(k-1)$ are annihilated the updated Cholesky square root factor is simply the first N rows of the resulting Givens rotated product,

$$\mathbf{C}^H(k) = \text{First N rows of } \mathbf{P}^H\mathbf{U}^H(k).$$

In order to calculate $\mathbf{P}^H\mathbf{U}^H(k)$, the N Givens rotations must be performed. Because of the form of the Givens premultiplier matrix, $\mathbf{P}_i^H$, only two rows of $\mathbf{U}^H(k)$ are altered at a time. Thus the updated Cholesky square root is formed by recomputing the i^{th} and $i+1^{st}$ rows of $\mathbf{U}^H(k)$ for i=1 to N. Because of the sparseness of the upper triangular matrix in $\mathbf{U}^H(k)$ this procedure requires very few numerical operations.

BEAMFORMING VECTOR GENERATION

As seen in Section 3.2 the MVDR beamformer requires that the inverse of the CSDM post multiplied by a known vector be computed in order to find the beamforming vector. This is seen by equation 3-25 to be,

$$\mathbf{w}(\theta) = \frac{N\mathbf{R}_p^{-1}\mathbf{A}^H\mathbf{d}(\theta)}{\mathbf{d}^H(\theta)\mathbf{A}\mathbf{R}_p^{-1}\mathbf{A}^H\mathbf{d}(\theta)}. \qquad 3\text{-}25$$

Note that the CSDM inverse post multiplied by the vector formed by the projection of the steering vector onto the presteering matrix appears in both the numerator and the denominator. Thus in order to form the beamforming vector the CSDM inverse post multiplied by $\mathbf{A}^H\mathbf{d}(\theta)$ need only be formed and placed into equation 3-25.

Forming the matrix-vector product as,

$$\mathbf{v} = \mathbf{R}^{-1}\mathbf{u}$$

where $\mathbf{u}$ is known and $\mathbf{v}$ is the desired output. Then multiplying both sides by the CSDM,

$$\mathbf{R}\mathbf{v} = \mathbf{u}.$$

Now replacing the CSDM by its Cholesky square root factorization as seen in equation A3,

$$\mathbf{C}\mathbf{C}^{H}\mathbf{v} = \mathbf{u}.$$

Let

$$\mathbf{r} = \mathbf{C}^{H}\mathbf{v} \qquad \text{A8}$$

where substitution yields,

$$\mathbf{C}\mathbf{r} = \mathbf{u}. \qquad \text{A9}$$

This equation (A9) may be solved for the unknown vector, $\mathbf{r}$, by a forward substitution. Once $\mathbf{r}$ is known, a backward substitution may be used to find the desired vector, $\mathbf{v}$, through equation A8. The forward and backward substitution algorithms are shown by Golub and Van Loan in [13]. They are used for the solution of the $\mathbf{A}\mathbf{x} = \mathbf{b}$ equation for $\mathbf{x}$ for lower and upper triangular matrices respectively.

The beamforming vector may now be computed with an overall order of N^2 numerical operations to accomplish the CSDM exponential update and the matrix inversion required by the MVDR beamformer.

APPENDIX B - Eigen-structure Estimation

INTRODUCTION

The enhanced minimum variance (EMVDR) beamformer requires the estimation of the D dominant eigenvectors and eigenvalues of the cross spectral density matrix (CSDM). This may be accomplished by a brute force general eigenvector decomposition routine performed on the exponentially averaged CSDM or by exploiting the structure of the CSDM and estimating only the eigenvectors that are desired. One of the algorithms that exploits the strucutre of the CSDM, as described in Section 3.1, is shown by Yang and Kaveh in [7].

The algorithm described in [7] also utilizes the fact that the eigenvectors of a matrix and of a polynomial function of the matrix are the same. The eigenvalues of the polynomial function of the matrix are the original eigenvalues operated on by the polynomial function. The particular polynomial function,

$$h(\mathbf{R}) = \mathbf{R}^{-1},$$

causes the eigenvectors corresponding to the D largest eigenvalues of $\mathbf{R}$ to be the D smallest eigenvalues of $h(\mathbf{R})$. Yang and Kaveh have shown that this particular estimation procedure performs better than the estimation of the D dominant eigenvectors of the non-inverted CSDM.

INITIALIZATION

Yang and Kaveh suggest initializing the estimate of the eigenvectors with the first D columns of an averaged CSDM where there must be at least D averages to provide enough linearly independent vectors. The first D columns are orthonormalized using the Gramm-Schmidt technique. It was found that initialization of the eigenvectors with an N-by-D identity matrix required many iterations of the algorithm for convergance near the true eigenvectors. Alternatively, as suggested by James Nuttall of NUSC, the eigenvectors may be initialized to the array steering vectors pointing to the direction of the D dominant sources. This method proved to work very well.

ALGORITHM

The algorithm required to perform the update is now presented in vector notation.

Iteration k:

Input: α - Averaging constant
$\mathbf{x}$ - Frequency data vector.
$\mathbf{w}_i(k-1)$ - Eigenvector estimates at time k-1, i=1, ..., D

Step 1: $\lambda_1 = \mathbf{w}_1^H(k-1)\mathbf{x}$

$$\mathbf{w}_p = (2\alpha-1)\mathbf{w}_1(k-1) + \frac{2(1-\alpha)\,\mathbf{x}\,\lambda_1^*}{\mathbf{x}^H\mathbf{x}}$$

$$\mathbf{w}_1(k) = \frac{\mathbf{w}_p}{\sqrt{\mathbf{w}_p^H\mathbf{w}_p}}$$

Step 2: Do j = 2 to D,

$\mathbf{x} = \mathbf{x} - \lambda_{j-1}\mathbf{w}_{j-1}(k)$

$\lambda_j = \mathbf{w}_j^H(k-1)\mathbf{x}$

$$\mathbf{w}_p = (2\alpha-1)\mathbf{w}_j(k-1) + \frac{2(1-\alpha)\,\mathbf{x}\,\lambda_j^*}{\mathbf{x}^H\mathbf{x}}$$

$$\mathbf{w}_j(k) = \frac{\mathbf{w}_p}{\sqrt{\mathbf{w}_p^H\mathbf{w}_p}}$$

End do

Output: $\mathbf{w}_i(k)$ - Eigenvector estimates at time k, i=1, ..., D
λ_i - Eigenvalue estimates, i=1, ..., D

APPENDIX C - Subarray Sizing Algorithm

INTRODUCTION

The size and spacing of a subarray is constrained to allow only a specified amount of aliasing and to utilize the full aperture of the array. For a given type of subarray shading each possible subarray size must be evaluated for validity in the above two concerns. The aliasing and full aperture usage constraints are elaborated on in Section 3.3.1.

This appendix is intended to introduce the algorithm used to compute the valid array size and spacing combinations when the array shading and the number of full array sensors is given. The scalloping loss limits, as described in Section 3.3.1.2, are found as well for the valid subarray size and spacing combinations.

DISCUSSION

The algorithm requires an educated searching routine that must locate the maximum point of the first sidelobe of the subarray beampattern generated by a given subarray size and shading. Once this is done the wavenumber in the mainlobe that has attenuation equal to that of the first sidelobe maximum is determined. From this value the subarray spacing is determined and tested to see if it is an integer. If it is an integer then the number of subarrays required to span the full array aperture is tested for an integer value characteristic. If both the integer constraints are satisfied the subarray size and spacing are a valid combination. The beampattern is then searched to find the wavenumber at which the scalloping loss limit is not violated. This will determine the number of subarray beams required to estimate the full arrival angle space (-90 to +90 degrees).

ALGORITHM

The algorithm is as follows:

Input:	N	- Number of sensors in full array
	wind(I)	- Subarray shading function, returns shading for I elements in column vector
	Scal	- Scalloping loss limit in dB

/* Loop through all possible subarray sizes (N_S = 3 to N-1) */
$N_{CNT} = 0$

```
N_S = 2
Step 1:     If (N_S<N-2) Then
      N_S = N_S + 1
      /* Get shadings for current subarray size */
      s = wind(N_S)
      /* Compute beampattern via FFT, convert to dB */
      bp = 10log10(abs(FFT(s,N_FFT))^2)

      /* Step through beampattern searching for scalloping
         loss limit, first minimum and first sidelobe
         maximum */

      /* Initialize for search */
      Iscal = 1
      B_MIN = False
      B_OLD = bp(1)
      I = 0
      Step 2:     I = I + 1
            /* Check for scalloping loss limit */
            If ((bp(I)<Scal) AND (Iscal=1)) Then
                  Iscal = Ind
            End if
            /* Check for first minimum */
            If ((bp(I)<B_CUR) AND (Q_MIN = False)) Then
                  Q_MIN = True
            Endif
            /* Check for first sidelobe maximum */
            If ((B_OLD>B_CUR) AND (Q_MIN = True)) Then
                  SLL = B_OLD
            Else
                  B_OLD = B_CUR
                  Goto Step 2
            Endif

      /* Find the aliasing point in the mainlobe */
      /* Initialize */
      I = 0
      Step 3:     I = I + 1
            If (bp(I)>SLL) Then
                  Goto Step 3
            Endif
            I_ALIAS = I
```

```
        /* Test for validity:  Integer constraints */
        Step 4:     N_A = N_FFT / 2I_ALIAS
                    M = 1 + (N - N_s)/N_A
                    If (M = Integer) Then
                         Goto Step 5
                    Else
                         Goto Step 1
                    End if

        /* Compute output parameters */
        Step 5:     N_CNT = N_CNT + 1
                    N_s(N_CNT) = N_s
                    M(N_CNT) = M
                    N_A(N_CNT) = N_A
                    L(N_CNT) = ceil(N_FFT/2I_SCAL)
                    Goto Step 1

Else
     Stop
Endif
```

Output:

N_s	- Vector of valid subarray sizes
M	- Vector of number of subarrays
N_A	- Vector of subarray spacings
L	- Vector of number of subarray beams
N_{CNT}	- Length of above vectors, number of valid combinations.

REFERENCES

[1] Owsley, N., Array Signal Processing, Ed. S. Haykin, Prentice-Hall, 1985.

[2] Owsley, N., "Systolic Array ABF," NUSC Tech. Rpt. 7981, 21 Sept. 1987.

[3] Gray, D. "Formulation of the Maximum SNR Array Processor in Beam Space," JASA, 72(4), October 1982.

[4] Owsley, N. and Abraham, D., "Preprocessing for High Resolution Beamforming," Proc. 23rd Asilomar Conference, 1 Nov. 1989, or NUSC Reprint Rpt. 8651.

[5] Owsley, N. Notes from EE300 Space-Time Signal Processing course given Spring 1989.

[6] Brogan, W., Modern Control Theory, Prentice-Hall,1985.

[7] Kaveh, M. and Yang, J., "Adaptive Eigensubspace Algorithms for Direction or Frequency Estimation and Tracking," IEEE Trans. on ASSP, Vol. 36, No. 2, Feb. 1988.

[8] Burdic, W., Underwater Acoustic System Analysis, Prentice-Hall, 1984.

[9] Marple, S., Digital Spectral Analysis with Applications, Prentice-Hall, 1987.

[10] Owsley, N., "Enhanced Minimum Variance Beamforming," in Underwater Acoustic Data Processing, Ed. Y. T. Chan, Kluwer Academic Publishers, 1989 or NUSC Tech. Rpt. 8305, 18 Nov. 1988.

[11] Owsley, N., "A Recent Trend in Adaptive Spatial Processing for Sensor Arrays: Constrained Adaptation," in Signal Processing, Ed. J. W. R. Griffiths et al., Academic Press, New York, 1973, pp.327-347.

[12] Van Veen, B., "An Analysis of Several Partially Adaptive Beamformer Designs," IEEE Trans. on ASSP, Vol. 37, No. 2, Feb. 1989.

[13] Golub, G. and Van Loan, F., Matrix Computations, Johns Hopkins University Press, 1989.

[14] Oppenheim, A. and Schafer, R., Digital Signal Processing, Prentice-Hall, 1975.

[15] Nuttall, A., "An Approximate FFT Technique for Vernier Spectral Analysis," NUSC Tech. Rpt. 4767, 16 Aug. 1974.

[16] Urick, R., Principles of Underwater Sound, McGraw Hill, 1983.

[17] Owsley, N., "A Constrained Gradient Search (CGS) Method with Application to Adaptive Sensor Arrays," NUSC Tech. Memo. 2242-207-69, 3 Sept. 1969.

[18] Frost, O., "An Algorithm for Linearly Constrained Adaptive Array Processing," Proc. of IEEE, Vol. 60, No. 8, Aug. 1972.

REDUCED DIMENSION ADAPTIVE BEAMFORMING (U)
D. A. Abraham, Surface Ship Sonar Department
TR #8747
31 July 1990
UNCLASSIFIED

DISTRIBUTION LIST

External:

NAVSEA 06UR (Dr. Y. Yam, R. Dostie)
OCNR/ONT, OCNR-231 (Mr. T. Goldsberry, N. Gerr)
DARPA NTO (Dr. C. Stuart, Dr. G. Mohnkern)
DTIC (2)
Analysis & Technologies, North Stonington, CT (D. Ghen, L. Gorham)
University of Connecticut, Storrs, CT (C. Knapp, P. Willett)